

Note: Contents of this paper should not be quoted or referred to without permission of the author(s).

Invited Book Chapter for the *Handbook on the Physics and Chemistry of the Rare Earths*

## **Filled Skutterudites**

Brian C. Sales

Solid State Division  
Oak Ridge National Laboratory, P.O. Box 2008  
Oak Ridge, Tennessee 37831-6030

“The submitted manuscript has been authored by a contractor of the U.S. Government under contract No. DE-AC05-00OR22725. Accordingly, the U.S. Government retains a nonexclusive, royalty-free license to publish or reproduce the published form of this contribution, or allow others to do so, for U.S. Government purposes.”

prepared by  
SOLID STATE DIVISION  
OAK RIDGE NATIONAL LABORATORY  
Managed by  
UT-BATTELLE, LLC  
under  
Contract No. DE-AC05-00OR22725  
with the  
U.S. DEPARTMENT OF ENERGY  
Oak Ridge, Tennessee

October 2002

# FILLED SKUTTERUDITES

Brian C. Sales

*Solid State Division, Oak Ridge National Laboratory,  
Oak Ridge, TN 37831-6056*

| Contents                                       | Page |
|--|------|
| 1. Introduction                                | 4    |
| 2. Structure                                   | 6    |
| 3. Lanthanide skutterudites as Zintl compounds | 8    |
| 4. Synthesis and crystal growth                | 10   |
| 5. La filled skutterudites                     | 12   |
| 6. Ce filled skutterudites                     | 18   |
| 7. Pr filled skutterudites                     | 22   |
| 8. Nd filled skutterudites                     | 29   |
| 9. Sm filled skutterudites                     | 30   |
| 10. Eu filled skutterudites                    | 31   |
| 11. Gd filled skutterudites                    | 32   |
| 12. Tb filled skutterudites                    | 33   |
| 13. Yb filled skutterudites                    | 33   |
| 14. Filled skutterudite thermoelectrics        | 35   |
| 15. Concluding Remarks                         | 42   |

## Symbols

|          |                                |
|----------|--------------------------------|
| ADP      | atomic displacement parameters |
| AFM      | antiferromagnetic metal        |
| BCS      | theory of superconductivity    |
| $B_{eq}$ | isotropic ADP                  |

|                  |   |
|------------------|---|
| C                | heat capacity                             |
| CEF              | crystalline electric field                |
| $C_{\text{RLM}}$ | heat capacity from resonant level model   |
| $C_{\text{ph}}$  | heat capacity from phonons                |
| dHvA             | de Hass-van Alphen                        |
| DOS              | density of states                         |
| $e_g$            | doubly degenerate 3d orbitals             |
| FIHFM            | field-induced heavy-fermion metal         |
| FMM              | ferromagnetic metal                       |
| H                | magnetic field                            |
| HFS              | heavy-fermion state                       |
| HFM              | heavy-fermion metal                       |
| HGS              | hybridization gap semiconductor           |
| HFSC             | heavy-fermion superconductor              |
| $k_B$            | Boltzmann constant                        |
| $\mathbf{k}$     | wavevector                                |
| LDA              | local density approximation               |
| M                | metal                                     |
| M-I              | metal to insulator transition             |
| $m_e$            | free electron mass                        |
| $m^*$            | effective electron mass                   |
| n-type           | electron doped semiconductor              |
| NFL              | non-Fermi liquid                          |
| ODS              | ordered state                             |
| P                | pressure                                  |
| p-type           | hole doped semiconductor                  |
| QCP              | quantum critical point                    |
| QO               | quadrupolar order                         |
| RRR              | residual resistance ratio                 |
| $R_W$            | Wilson-Sommerfeld ratio                   |
| S                | Seebeck coefficient                       |
| SC               | superconductor                            |
| T                | temperature                               |
| T                | magnetic field in Tesla                   |
| $T_{\text{AF}}$  | antiferromagnetic ordering temperature    |
| $T_c$            | superconducting transition temperature    |
| $T_{\text{co}}$  | cold temperature of thermoelectric device |
| $T_d$            | displacive ordering transition            |
| $T_{\text{FM}}$  | ferromagnetic ordering temperature        |
| $T_{2g}$         | triply degenerate 3d orbitals             |
| $T_h$            | hot temperature of thermoelectric device  |
| $T_k$            | Kondo temperature                         |
| $T^*$            | characteristic temperature                |
| $T_o$            | characteristic temperature                |
| $\mu_B$          | Bohr magneton                             |

|                       |  |
|-----------------------|--|
| $\mu_{\text{eff}}$    | effective magnetic moment                    |
| XANES                 | x-ray absorption near edge spectroscopy      |
| Z                     | thermoelectric figure of merit               |
| ZT                    | dimensionless thermoelectric figure of merit |
| $\gamma$              | electronic coefficient of heat capacity      |
| $\Gamma$              | $(1+ZT)^{1/2}$                               |
| $\Gamma_1$            | crystal field singlet                        |
| $\Gamma_3$            | non-Kramers doublet (crystal field state)    |
| $\Gamma_4$            | crystal field triplet                        |
| $\Gamma_5$            | crystal field triplet                        |
| $\Delta$              | hybridization gap                            |
| $\Delta C$            | jump in heat capacity at $T_c$               |
| $\kappa$              | total thermal conductivity of solid          |
| $\kappa_e$            | thermal conductivity of electrons or holes   |
| $\kappa_L$            | thermal conductivity of lattice              |
| $\kappa_{\text{min}}$ | minimum lattice thermal conductivity         |
| $\rho$                | electrical resistivity                       |
| $\Theta_D$            | Debye temperature                            |
| $\chi$                | magnetic susceptibility                      |
| $\chi_0$              | magnetic susceptibility at $T = 0$           |

## 1. Introduction

Skutterudite is the name of a  $\text{CoAs}_3$  -based mineral that was first extensively mined as a source of cobalt and nickel in the region of Skutterud Norway. Compounds with the same cubic crystal structure have since been known as “skutterudites”. Oftedal first extensively studied the skutterudite crystal structure in 1928. An example of a well-formed natural skutterudite mineral is shown in fig. 1.

The skutterudite structure has two voids in each unit cell that are large enough to accommodate a variety of atoms including most of the light rare earth lanthanides ( La,Ce,Pr, Nd, Sm, Eu, Gd,Tb) and Yb. The first “filled skutterudites” were synthesized by Professor Jeitschko and collaborators in the late 1970’s (Jeitschko and Braun 1977, Braun and Jeitschko 1980a,b, c). The chemical composition of the lanthanide filled skutterudites is given by  $\text{RM}_4\text{X}_{12}$ , where R are the



Fig. 1. Photograph of a natural skutterudite mineral. This extremely well crystallized specimen is from the Sandroste Mine near Bou Azzer, Morocco. (Image downloaded from Carnegie-Mellon Mineral Collection Images, Alan Guisewite's collection)

lanthanides noted above,  $M = \text{Fe, Ru, Os}$  and  $X = \text{P, As, Sb}$ . For each lanthanide element there is a maximum of nine distinct compounds with the skutterudite structure. In 1996 it was found that some of the lanthanide skutterudites had excellent thermoelectric properties above room temperature (Sales 1996, Fleurial 1996) and this greatly increased the interest in these materials for thermoelectric applications. In addition to the stoichiometric filled skutterudite compounds of the form  $\text{RM}_4\text{X}_{12}$ , a large number of related alloys were also investigated as possible thermoelectric materials. Most of the research on lanthanide skutterudites in the context of thermoelectric applications has been reviewed recently by Uher (1999), Nolas et al. (1999), and Sales (1998) and hence only a brief summary of the thermoelectric research will be presented at the end of this article. This chapter will focus on what is known about the structural, electronic and magnetic properties of the stoichiometric lanthanide skutterudite compounds of the form  $\text{RM}_4\text{X}_{12}$ . The low temperature properties will be of particular interest since these compounds exhibit a rich variety of electronic and magnetic ground states that include heavy-fermion-mediated superconductivity, ferromagnetism, antiferromagnetism, hybridization gaps (Kondo

insulator behavior), non-Fermi-liquid behavior and quantum critical points, quadrupolar ordering, and field-induced heavy-fermion states.

## 2. Structure

The filled skutterudites crystallize in the cubic space group  $Im\bar{3}$  with two formula units ( $RM_4X_{12}$ ) per unit cell. There are three unique atomic positions in the normalized unit cell. The rare earth position is (0,0,0), the transition metal position is (0.25, 0.25, 0.25), and the pnictogen (P, As, Sb) position (0, y, z) is variable with  $y \approx 0.35$ ,  $z \approx 0.16$  (fig. 2). The positions of the

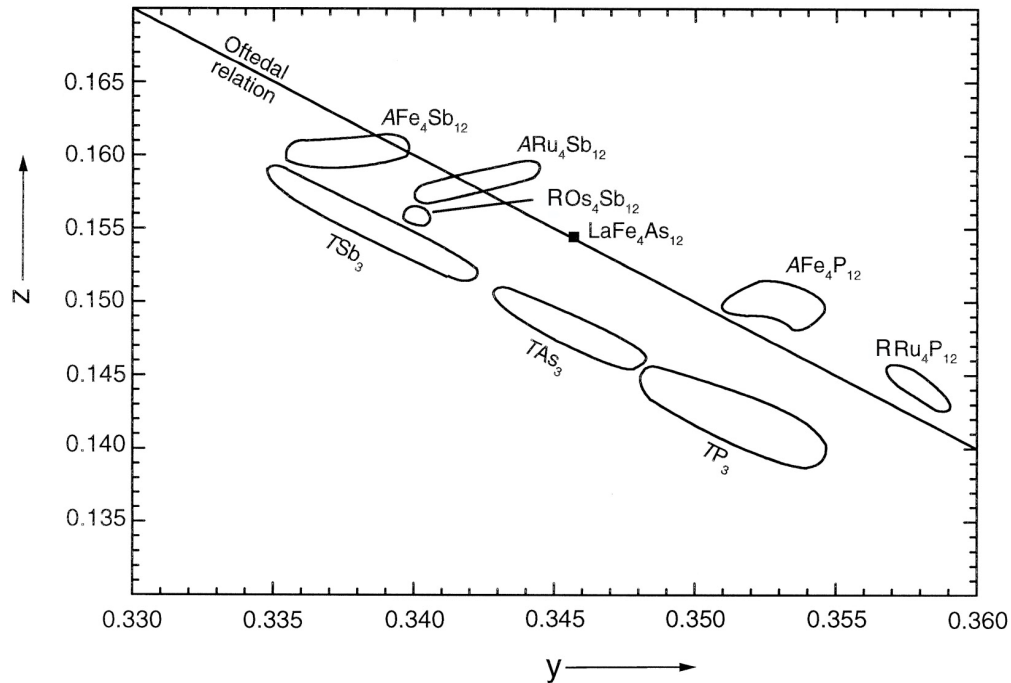


Fig. 2. Positional parameters for the pnictogen atoms of filled and unfilled skutterudites (figure from Kaiser and Jeitschko 1999). The straight line indicates the condition for square pnictogen rings. In the figure T= Co, Rh or Ir; A = light lanthanides or Yb, Ca, Sr or Ba; R = light lanthanides.

remaining 31 atoms in the unit cell are determined by the symmetry operations associated with the  $Im\bar{3}$  space group (fig 3). As has been reviewed in detail by Uher (1999), the exact values of y and z for the unique pnictogen position depend on the particular compound, and reflects the fact the pnictogen rings (fig. 4) in the structure are not exactly square and the  $MX_6$  octahedra are slightly distorted. If the pnictogen rings were exactly square and the octahedra symmetric, the

pnicogen position would reduce to  $(x=0, y=0.25, z=0.25)$ . The similarities between the filled-

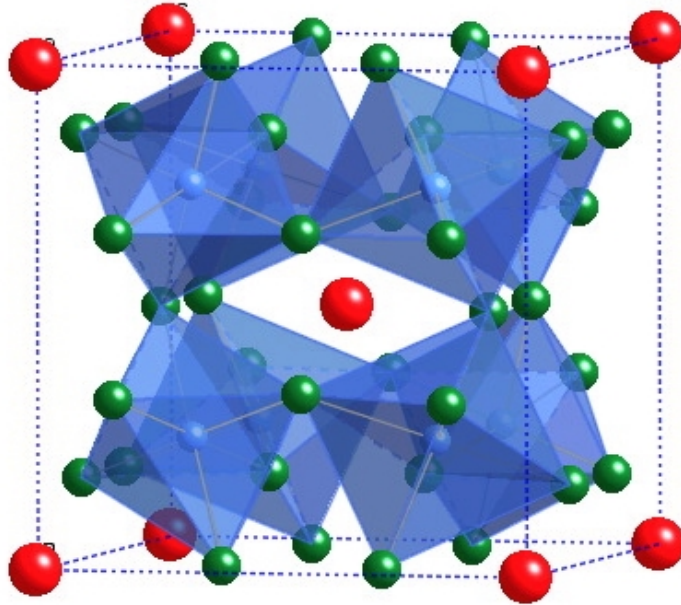


Fig. 3. Model of the filled skutterudite structure. The transition metal atoms (Fe, Ru, or Os -small light blue spheres) are at the center of distorted octahedra formed by the pnictogen atoms (P, As, Sb- green spheres). The lanthanide atoms (red spheres) are located at the center of a cage formed by 12 pnictogen atoms. The skutterudite structure results if the lanthanide atoms are removed from the structure and the transition metals (Fe, Ru or Os) are replaced by transition metals with one more outer shell electron (Co, Rh or Ir).

skutterudite structure and the more familiar perovskite (e.g.  $\text{CaTiO}_3$ ) and  $\text{ReO}_3$  structures have been discussed by Jeitschko and Braun 1977. In the ideal perovskite structure the eight octahedra are not tilted which results in eight voids that are filled by Ca atoms. The tilting of the octahedra in the skutterudite structure reduces the volume of six of these voids which become the centers of rectangular pnictogen ( $\text{P}_4$ ,  $\text{As}_4$  or  $\text{Sb}_4$ ) groups. The remaining two voids are greatly enlarged and can accommodate lanthanide atoms (fig. 4). Each lanthanide atom is located at the center of a distorted icosahedron formed by 12 pnictogen atoms. The size of this icosahedral cage formed by the pnictogen atoms increases as the pnictogen is changed from P to As to Sb. In many of the antimonide compounds the atomic displacement parameters for the lanthanide atoms are unusually large, indicating substantial “rattling” of the R atoms about their equilibrium positions

and poor bonding to the antimony atoms forming the cage (Braun and Jeitschko 1980a, Kaiser and Jeitschko 1999). The filled skutterudite structure does not form with the smaller lanthanide elements (Dy-Tm) or Y or Sc because the pnictogen cage is too large for the necessary lanthanide-pnictogen bonding.

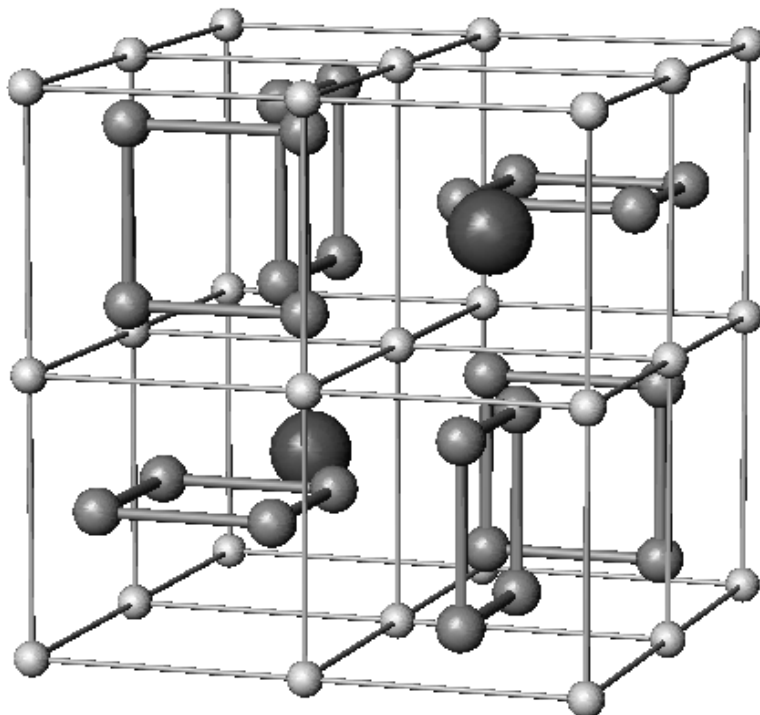


Fig. 4. Model of filled-skutterudite structure that emphasizes the pnictogen-pnictogen bonding that results in nearly square pnictogen rings. The transition metal atoms (small white spheres) form a simple cubic lattice as shown. The lines connecting the transition metal atoms have been added for clarity and do not correspond to a chemical bond. The only chemical bonds shown in this model are those that form the pnictogen rings. The lanthanide atoms (large dark spheres) occupy the two voids without a pnictogen ring.

### 3. Lanthanide skutterudites as Zintl compounds

The qualitative electronic structure of the filled skutterudites can be understood within the framework of the Zintl concept (for a good discussion of Zintl's ideas see Corbett 1985, Mueller 1993). Zintl phases are characterized by the presence of covalently bonded anion structures similar to those found in the pure element. In the skutterudites, the pnictogen rings can be considered Zintl anions. The strongly electropositive cations (lanthanide elements and to a lesser extent the transition metal atoms), simply provide the necessary charge to complete the outer

electron shell of the pnictogen anions. The Zintl concept can be applied to a huge number of compounds containing elements from the IVB, VB and VIB columns of the periodic table. Zintl compounds tend to be small gap semiconductors or bad metals. For the unfilled skutterudites, such as  $\text{CoSb}_3$ , each Sb atom is bonded to two Sb and two Co atoms, and each Co atom is bonded to six Sb atoms (figs. 3 and 4). The outer shell of each Sb atom is  $5s^2p^3$  and so to attain a closed shell ( $5s^2p^6$ ) requires 3 electrons. The two covalent Sb-Sb bonds provide two of the electrons. The third electron is donated by the two Co atoms (a half an electron from each). This argument suggests that Co should have a formal valence of +3. In an octahedral site, the crystal field will result in a splitting of the five Co 3d orbitals into a ground state triplet ( $t_{2g}$ ) and an excited state doublet ( $e_g$ ). (For an exceptionally clear discussion of why this occurs see Mueller 1993). The six d electrons of  $\text{Co}^{+3}$  can completely occupy the  $t_{2g}$  orbital with no net magnetic moment, which is consistent with the measured diamagnetism for  $\text{CoSb}_3$ . This argument would also suggest that  $\text{CoSb}_3$  is a semiconductor. Although the simple Zintl concept appears to work for  $\text{CoSb}_3$ , it is important to realize that the Zintl picture is only a guideline and like many of the most useful guidelines they often work but sometimes they do not. In the case of  $\text{CoSb}_3$  it is not clear that the Zintl picture should work well since there is not much difference in electronegativity between Co (1.88) and Sb (2.05). Detailed electronic structure calculations (Singh and Pickett 1994, Sofo and Mahan 1998) indicate that the electronic structure of  $\text{CoSb}_3$  is rather complicated with a small gap of 0.05 eV at the Fermi energy due to a single band that crosses a much larger pseudogap (0.8 eV) between the valence and conduction bands.

The electronic structure of the lanthanide filled skutterudites can also be analyzed using the Zintl picture. The lanthanide filled skutterudites (e.g.  $\text{LaFe}_4\text{Sb}_{12}$ ) form with the transition metals Fe, Ru or Os. These elements have one less outer electron relative to the elements in the next column of the periodic table (Co, Rh, or Ir). If the lanthanide elements contribute three electrons toward satisfying the bonding requirements of the pnictogen atoms, the total electron count is satisfied if each transition metal contributes on average 2.25 electrons. Although in terms of electron count an average valence of 2.25 should result in a semiconductor (within the Zintl picture), an average valence of 2.25 at each transition metal site would also imply a partially filled d band near the Fermi level. Since each transition metal is at a crystallographically equivalent site there is no reason to assume a spatial distribution of different transition metal valence states. This simple argument would suggest that all of the lanthanide filled

skutterudites should be poor metals. If the transition metal has an integer valence of +2, then a better metal should result with holes as the dominant carriers. For most of the lanthanide skutterudites the Zintl picture seems to be qualitatively correct at least as a starting point for understanding the electronic properties of these compounds. These simple ideas are useful but should only be regarded as guidelines and not a substitute for a modern electronic structure calculation. For example, density functional calculations of the electronic structure of  $\text{CeFe}_4\text{Sb}_{12}$ , and  $\text{CeFe}_4\text{P}_{12}$  indicate that both compounds are small band gap semiconductors (Nordstrom and Singh 1996). The gap is due to strong hybridization between the Ce 4f level and Fe 3d and pnicogen states near the Fermi energy.

#### **4. Synthesis and crystal growth**

The skutterudites do not melt congruently and involve pnicogens (P, As, Sb) that generally have high vapor pressures at the formation temperatures of the compounds. The high melting temperatures of Fe, Ru and Os coupled with the reactivity of the lanthanide metals with convenient crucible materials (e.g.  $\text{SiO}_2$ ) makes the synthesis of many of these compounds difficult. As a result, variations in the reported properties of a particular lanthanide skutterudite compound can often be traced to differences in sample composition and quality.

Small single crystals of most of the lanthanide phosphides can be grown in a molten tin flux (Jeitschko and Braun 1977, Meisner 1981, Meisner et al. 1985, DeLong and Meisner 1985, Torikachvili et al. 1987, Watcharapasorn et al. 1999, Sato et al. 2000a,b). For example,  $\text{LaFe}_4\text{P}_{12}$  crystals were grown using La filings, Fe powder, red phosphorus and Sn in the atomic ratio 1:4:20:50. The mixture was sealed in an evacuated silica tube, annealed for one week at 1050 K, and slow cooled (2K/h) to about 773 K, followed by rapid cooling to room temperature. A 1:1 mixture of HCl and water was then used to dissolve the Sn flux (Jeitschko and Braun 1977). Single crystals with typical dimensions from 0.1-2 mm can be grown by this method. Although this recipe clearly works and has been used by several authors, it may not be the optimum procedure for growing the largest phosphide crystals based on the known binary phase diagrams. A larger concentration of Sn and a carbonized silica tube along with larger pieces of lanthanide metals and cooling to lower temperatures might result in larger phosphide crystals. Polycrystalline skutterudite phosphides have also been synthesized directly from the elements using a high pressure (4 GPa) and high temperature (800-1200 °C) wedge-type cubic-anvil

apparatus (Shirotani et al. 1996, Shirotani et al. 1997, Sekine et al. 1997, and Uchiumi et al. 1999). This technique avoids contamination from residual Sn flux.

Lanthanide arsenides with the filled skutterudite structure were prepared by Braun and Jeitschko 1980b. Lanthanide arsenides, RAs, were first prepared by reacting lanthanide filings with As in a silica tube at 900 K for 2 days. The RAs material was then ground together with the transition metal and excess As (R: T: As = 1:4:20) and sealed again in evacuated silica tubes, rapidly heated to 1150 K and kept at temperature for 3h. The samples were then annealed at 1000 K for 4-7 days. The excess As was removed through sublimation. In spite of this elaborate synthesis procedure, the overall products were only 70-90% single phase. However, small single crystals of the skutterudite phase suitable for x-ray structure refinement could often be isolated from the reaction product. A dense single phase sample of  $\text{CeFe}_4\text{As}_{12}$  was prepared by a similar procedure followed by the densification of the powder with a hot-press (Watcharapasorn et al. 2002). Single phase arsenides with a variety of compositions have also been prepared via direct high-pressure high-temperature synthesis from the elements (Shirotani et al. 1997).

Synthesis of the lanthanide antimonides with the filled skutterudite structure have been investigated in much more detail than either the arsenides or phosphides because of the excellent thermoelectric properties of these materials at elevated temperatures. These materials were first synthesized by Braun and Jeitschko 1980a using a procedure similar to that described above for the synthesis of the arsenides. The phase purity of the antimonides prepared in this manner was only about 80%. A better synthesis procedure was reported Sales et al. 1996, 1997. A thin layer of carbon was deposited on the inside of a round-bottomed silica tube by the pyrolysis of acetone. Stoichiometric amounts of high purity lanthanide metal pieces (99.99% electropolished bar from Ames laboratory), Fe rod (99.9985% from Alfa Chemical Company), and Sb shot (99.999% from Alfa) were loaded into the precarbonized tube. The tube was sealed under vacuum at a pressure of  $10^{-3}$  Pa and transferred into a programmable furnace. The silica ampoule was heated to 600°C at 2°C/min, left at 600 °C for 3 h, and then slowly (0.5 °C/min) heated to 1050 °C and left for about 20-40 h. It is important to slowly heat the tube because of the highly exothermic reaction between the lanthanide elements (particularly Ce) and antimony. The silica ampoule containing the homogeneous molten liquid was removed from the furnace at temperature and quenched into a water bath. The same ampoule (containing the prereacted elements) was then placed in a furnace and annealed at 700 °C for 30 h to form the correct

crystallographic phase. The completely reacted solid was removed from the silica tube and cleaned with a wire brush to remove small amounts of carbon from the surface. To form a completely dense polycrystalline solid, the reacted material was ball milled into a fine powder in an argon atmosphere, loaded into a graphite die, and hot-pressed (5000 psi) in a helium atmosphere at 700°C for 40 mins. This procedure results in single phase and dense polycrystalline samples suitable for further investigation (transport, magnetic, optical etc.) Single crystals of the antimonides can also be grown using excess antimony as a flux (Chakoumakos et al. 1999, Takeda and Ishikawa 2000b, Bauer, E. D. et al. 2001a, b). High purity elements in the ratio R: T: Sb = 1:4:20 are loaded into an evacuated carbon coated quartz tube. The tubes are heated to 900°C for 24 h and then cooled slowly (1-3 °C/h) to 600 °C, followed by a quench to room temperature. The excess Sb flux can be removed by etching in acid (HCl: HNO<sub>3</sub> = 1:1). Small quantities of new compounds with the skutterudite structure can also be synthesized using a clever non-equilibrium thin film method pioneered by D. C. Johnson and collaborators at the University of Oregon (Hornbostel et al. 1997a, 1997b). The new compounds are formed by the low-temperature interdiffusion of multilayer elemental reactants.

### 5. La filled skutterudites

**LaFe<sub>4</sub>P<sub>12</sub>** is a metal that becomes superconducting for temperatures below 4.1 K (Meisner 1981). The residual resistance ratio (RRR) for these crystals is large RRR= 90 –1500 indicating good crystallographic perfection (Torikachvili et al. 1987, Sato et al. 2000a,b, Sugawara et al. 2000). The resistivity at room temperature is about 250 μΩ-cm (Sugawara et al. 2000) in fair agreement with optical conductivity data which yields a value of 85 μΩ-cm (Dordevic et al. 1999). Superconductivity is rare in compounds that contain such high concentrations of iron. Mössbauer measurements found that each iron atom in LaFe<sub>4</sub>P<sub>12</sub> carried a magnetic moment less than 0.01μ<sub>B</sub> (Shenoy et al. 1982, Grandjean et al. 1984). The magnetic susceptibility data is weakly temperature dependent and saturates below 50 K at a value of 8 x 10<sup>-4</sup> cm<sup>3</sup>/mole (emu/mole) (Meisner 1981, Grandjean et al. 1984). If the iron moments are in a low spin configuration similar to Fe<sup>+2</sup>, from the Zintl picture discussed in sect. 3, the compound should be a hole doped metal. Hall measurements (Sato et al. 2000b) and band structure calculations (Harima 1998) both indicate hole like conduction. Band structure predicts two hole-like Fermi sheets, a nearly spherical sheet composed mainly of Fe 3d states and a multiply connected sheet of mainly P-p character (fig 5). The band structure calculations are in good agreement with the

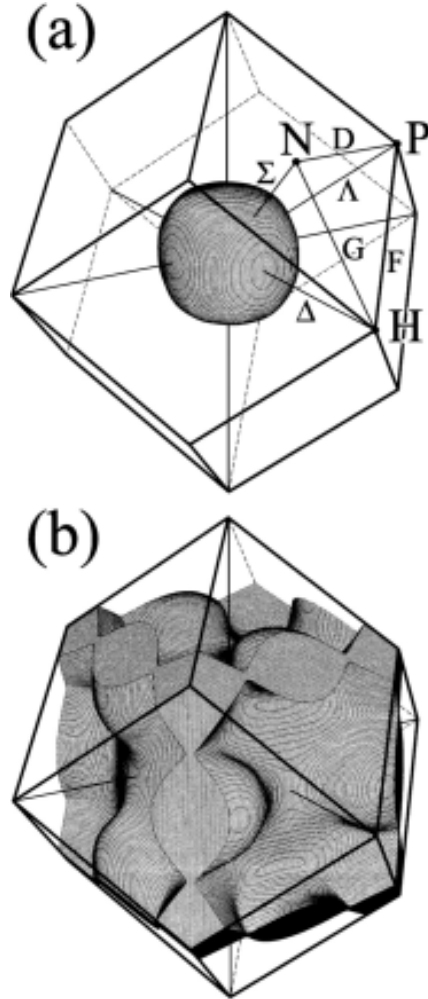


Fig. 5. The Fermi surface of  $\text{LaFe}_4\text{P}_{12}$  consists of two hole-like Fermi sheets. The first sheet (a) is nearly spherical with mainly Fe 3d character while the second sheet (b) is multiply connected with mainly P-p character. Both surfaces are centered at the  $\Gamma$  point. Various high-symmetry directions are noted in (a). (Harima 1998, Sugawara et al. 2000).

two masses extracted from dHvA measurements on  $\text{LaFe}_4\text{P}_{12}$  crystals (Sugawara et al. 2000). The predicted electronic specific heat coefficient,  $\gamma$ , from the band structure calculations, was  $32 \text{ mJ/mole-K}^2$  in fair agreement with the experimental value of  $57 \text{ mJ/mole-K}^2$  (Torikachvili et al. 1987). The relatively high density of electronic states and the absence of magnetism suggests that  $\text{LaFe}_4\text{P}_{12}$  is a relatively normal BCS superconductor. The jump in the heat capacity at  $T_c = 4.1 \text{ K}$  is about 87% of the value expected from BCS theory.

**$\text{LaRu}_4\text{P}_{12}$**  is a metal that superconducts below  $7.2 \text{ K}$  (Meisner 1981, Delong and Meisner 1985, Uchiumi et al. 1999). The room temperature resistivity of a polycrystalline sample was  $600 \mu\Omega\text{-cm}$  decreasing to about  $20 \mu\Omega\text{-cm}$  at  $8 \text{ K}$  (Shirotani et al. 1996). Analysis of the low

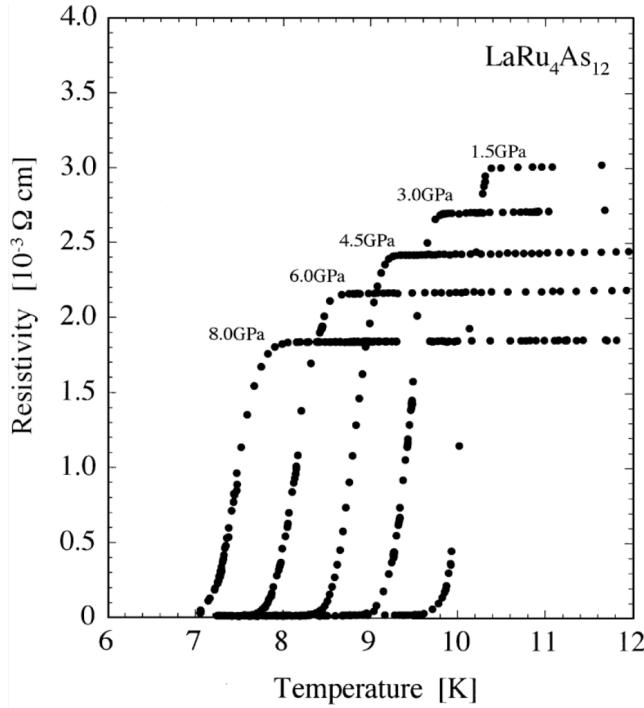


Fig. 6. Electrical resistivity of  $\text{LaRu}_4\text{As}_{12}$  versus temperature and pressure (Shirotani et. al 2000).

temperature heat capacity data yields  $\gamma = 26 \text{ mj/mole-K}^2$  and a Debye temperature,  $\Theta_D = 446 \text{ K}$ . The magnetic susceptibility is essentially temperature independent from 7-300 K, consistent with Pauli paramagnetism (Uchiumi et al. 1999).

$\text{LaOs}_4\text{P}_{12}$  is a metal with a room temperature resistivity of about  $400 \mu\Omega\text{-cm}$ , which decreases to  $50 \mu\Omega\text{-cm}$  at 2 K followed by superconductivity at 1.8 K (Shirotani et al. 1996, Meisner 1981). There is a weak decrease of  $T_c$  with increasing pressure (DeLong and Meisner 1985).

$\text{LaFe}_4\text{As}_{12}$  is a metal that shows a monotonic decrease in resistivity down to 2 K with no evidence of superconductivity (Shirotani et al. 2000).

$\text{LaRu}_4\text{As}_{12}$  is a poor metal with the highest superconducting transition temperature (10.3 K) of all of the filled skutterudites. Polycrystalline samples can be prepared using high pressure and high temperature (Shirotani et al. 1996, 1997, 2000, Uchiumi et al. 1999). The resistivity at room temperature is  $13 \text{ m}\Omega\text{-cm}$  decreasing to  $3 \text{ m}\Omega\text{-cm}$  at 12 K. The temperature dependence of the resistivity exhibits a large positive curvature that suggests substantial structure in the electronic density of state near the Fermi energy. Low temperature heat capacity measurements yield  $\gamma = 73 \text{ mj/mole-K}^2$ , and  $\Theta_D = 233 \text{ K}$ . The normalized jump in the heat capacity at  $T_c$  is 1.75 which is

slightly larger than the BCS value of 1.43. With increasing pressure  $T_c$  decreases at the rate  $dT_c/dP = -0.4$  K/GPa (fig. 6)

**LaOs<sub>4</sub>As<sub>12</sub>** is metallic exhibiting superconductivity below 3.2 K (Shirotani et al. 2000). The resistivity (polycrystalline sample) at room temperature is 0.8 mΩ-cm decreasing to 0.1 mΩ-cm at 4 K.

**LaFe<sub>4</sub>Sb<sub>12</sub>** is a poor metal or heavily doped semiconductor with good thermoelectric properties above room temperature (700-1000 K) (Sales et al. 1996, 1997). Only polycrystalline samples have been investigated. The room temperature resistivity is about 0.5 mΩ-cm decreasing to 0.1 mΩ-cm at 10 K. The typical carrier concentration estimated from room temperature Hall data is  $2 \times 10^{21}$  holes/cm<sup>3</sup>. The Seebeck coefficient,  $S$ , at room temperature is +75 μV/K which is typical for a heavily doped semiconductor (the value of  $S$  for a good metal is usually less than 10 μV/K in magnitude). The electronic structure near the Fermi energy has more than one type of band since the Seebeck coefficient changes sign near 100 K (fig. 7). There has been no report of superconductivity in this material above 2 K. There is no evidence of long range magnetic order. The magnetic susceptibility indicates some type of enhanced paramagnetism that is probably associated with nearly itinerant 3d electrons (D. Ravot et al. 2001, Dannebrock et al. 1996, Sales unpublished). Although the temperature dependence of the susceptibility is similar for all three samples, the magnitude of the room temperature susceptibility varies substantially from 0.0019 emu/mole (Ravot et al. 2001) to 0.004 (Dannebrock et al. 1996- note that all of the susceptibility data in Dannebrock's fig. 2 appears to be mislabeled since the susceptibility values are too high by a factor of 10). At helium temperatures the susceptibility saturates for all three samples near 0.02 emu/mole. Probably the best interpretation of the susceptibility data was given by Ravot et al. (2001) who were able to account for the nearly Curie-Weiss dependence of the susceptibility in terms of a Stoner band picture. This interpretation is also consistent with the discussion in sect. 3, which implies some type of band magnetism if the average iron valence is 2.25. However, the significant variation of the susceptibility from sample to sample and the difficulty in ruling out small amounts (<3%) of a magnetic impurity phase suggests that the magnetism may not be intrinsic to the skutterudite phase. Susceptibility measurements should be repeated using a single crystal free of impurity phases.

Braun and Jeitschko (1980a) noted that the lanthanide site in the antimonides is too large for La, the largest trivalent lanthanide element. The poor bonding of La to the surrounding antimony

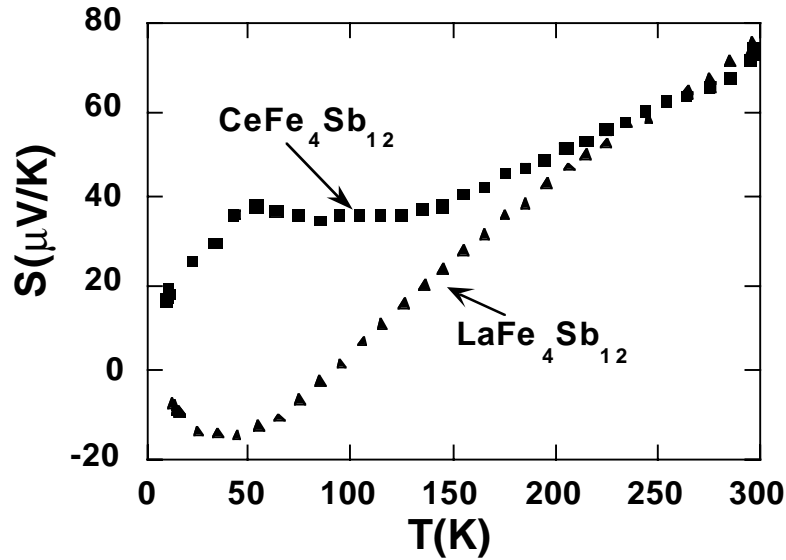


Fig. 7 Seebeck coefficient vs. temperature for  $\text{LaFe}_4\text{Sb}_{12}$  and  $\text{CeFe}_4\text{Sb}_{12}$  (Sales et al. 1997, unpublished)

atoms results in a large atomic displacement parameter (ADP) for La and corresponds to the La “rattling” about its equilibrium position. As a first approximation the rattling La atom can be treated as a localized Einstein oscillator. Slack (1995) was first to suggest that if the frequency of the Einstein oscillator is low enough, it could result in a substantial reduction in the lattice thermal conductivity of the filled skutterudites by hybridizing with the acoustic phonons that carry the majority of the heat in most solids. This idea has been experimentally verified by many authors (Morelli and Meisner 1995, Sales et al. 1996, Fleurial et al. 1996, Nolas et al. 1996a,b, Nolas et al 1998, Sales et al. 1997, Morelli et al. 1997, Meisner et al. 1998, Sales et al. 2000, Sales et al. 2001a,b). A low lattice thermal conductivity,  $\kappa_L$ , is necessary for a good thermoelectric material. The room temperature value of  $\kappa_L$  for dense polycrystalline  $\text{LaFe}_4\text{Sb}_{12}$  is approximately 1.5 W/m-K. An estimate of the Einstein frequency for La in  $\text{LaFe}_4\text{Sb}_{12}$  has been obtained from heat capacity, elastic constant, inelastic neutron scattering (fig. 8), ADP data and theory (Sales et al 1997, Keppens et al. 1998, Sales et al. 1999, Feldman et al. 2000). All of the measurements indicate a characteristic Einstein temperature of about 75 K for the La atoms.

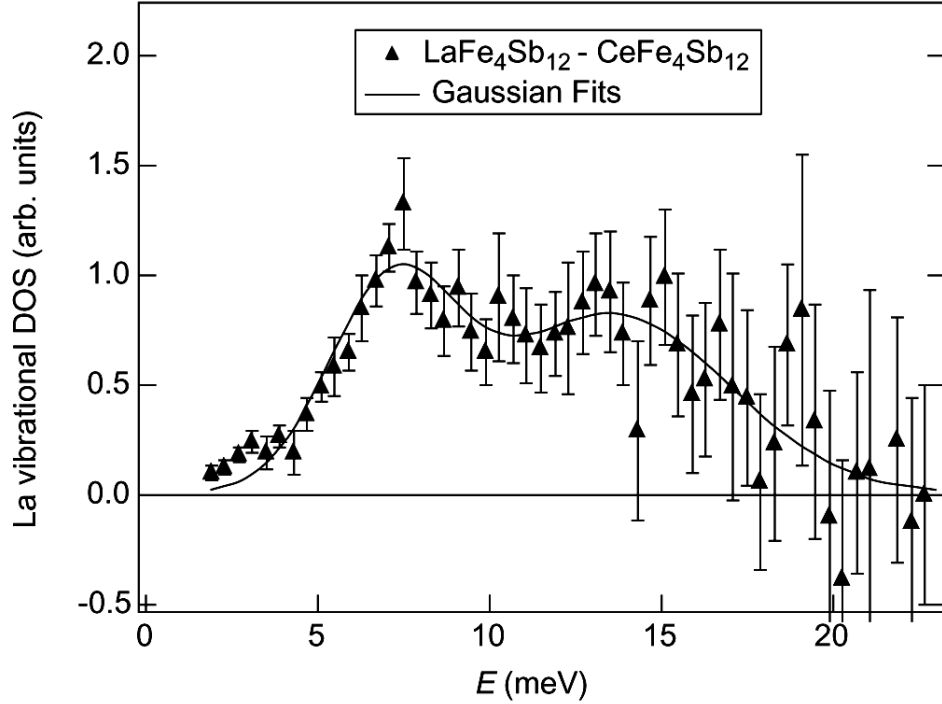


Fig. 8 Difference in the inelastic neutron scattering data between  $\text{LaFe}_4\text{Sb}_{12}$  and  $\text{CeFe}_4\text{Sb}_{12}$  versus energy loss (Keppens et al. 1998).  $\text{CeFe}_4\text{Sb}_{12}$  was used as a reference compound since the neutron scattering cross section of Ce is much smaller than that of La. The difference spectra therefore reflect the vibrational density of states (DOS) associated with the La atoms. The peak at 7 meV (78 K) corresponds to the quasi-localized La mode. The second broader peak at about 15 meV corresponds to the hybridization of La and Sb vibrational modes. Both peaks can be accounted for using lattice dynamic models based on first-principles calculations (Feldman et al. 2000).

$\text{LaRu}_4\text{Sb}_{12}$  is metallic and is superconducting below about 3.6 K (Uchiumi et al. 1999, Takeda and Ishikawa 2000b, E. D. Bauer et al. 2001a). Low temperature heat capacity data yield  $\gamma = 37 \text{ mJ/mole-K}^2$ , and  $\Theta_D = 253 \text{ K}$ . The residual resistivity ratio (RRR) is about 69 for the small crystals but no absolute values for the resistivity are reported (Takeda and Ishikawa 2000b). Polycrystalline samples synthesized at high pressures have a resistivity of  $0.7 \text{ m}\Omega\text{-cm}$  and a much smaller RRR of 7. The  $T_c$  of the polycrystalline material is also significantly lower (2.8 K) (Uchiumi et al. 1999). The normalized jump in the heat capacity at  $T_c$  is 2.22, which suggests that  $\text{LaRu}_4\text{Sb}_{12}$  is a superconductor with moderate coupling (Takeda and Ishikawa 2000b). The room temperature magnetic susceptibility of  $\text{LaRu}_4\text{Sb}_{12}$  is diamagnetic with a value of  $-1.93 \times 10^{-4} \text{ emu/mole}$ .

**LaOs<sub>4</sub>Sb<sub>12</sub>** is presumably a metal although only heat capacity data from small single crystals have been published resulting in  $\gamma = 36$  mJ/mole-K<sup>2</sup> and  $\Theta_D = 304$  K. There is no evidence for superconductivity above 0.5 K (E. D. Bauer et al. 2001b).

## 6. Ce filled skutterudites

**CeFe<sub>4</sub>P<sub>12</sub>** is a small gap semiconductor with the gap likely arising from the hybridization of the Ce 4f states with the Fe 3d and P p states in the vicinity of the Fermi energy (Meisner et al. 1985, Nordstrom and Singh 1996). The susceptibility of CeFe<sub>4</sub>P<sub>12</sub> is small ( $2.6 \times 10^{-4}$  emu/mole), and is roughly a factor of 2 less than its non-magnetic analog LaFe<sub>4</sub>P<sub>12</sub>. The lattice constant of CeFe<sub>4</sub>P<sub>12</sub> (7.792 Å) is significantly smaller than would be expected for trivalent Ce based on the values for LaFe<sub>4</sub>P<sub>12</sub> (7.8316 Å) and PrFe<sub>4</sub>P<sub>12</sub> (7.8149 Å). The susceptibility data and the lattice constant suggest the possibility of Ce<sup>+4</sup>. However, XANES (X-ray absorption near edge spectroscopy) measurements (Xue et al. 1994) clearly indicate that the Ce is primarily trivalent, though with some evidence of complex electronic behavior. The resistivity increases with decreasing temperature but the behavior is complicated and somewhat sample dependent (Meisner et al. 1985, Sato et al. 2000b). Analysis of single crystal resistivity data above 250 K gives a transport gap of about 0.12 eV (Sato et al., 2000b) which is close to the value of 0.15 eV measured from infrared reflectance spectroscopy (Dordevic et al. 1999). Both values are somewhat smaller than the value of 0.34 eV calculated within the local-density approximation (LDA) (Nordstrom and Singh 1996). The temperature dependence of the Hall coefficient from 2-300 K appears to be reproducible from crystal to crystal but is difficult to interpret (Sato et al. 2000b). The Seebeck coefficient at room temperature is large for single crystals ( $\approx 0.5$  mV/K) (Sato et al. 2000b) but is about 10 times smaller in hot-pressed polycrystalline samples with small amounts of impurity phases (Watcharapasorn et al. 1999). The room temperature thermal conductivity of a polycrystalline sample is 14 W/m-K, which is about ten times larger than the typical values of good thermoelectric materials (Watcharapasorn et al. 1999).

**CeRu<sub>4</sub>P<sub>12</sub>** is a narrow gap semiconductor with a gap of 0.075 eV estimated from electrical transport measurements on polycrystalline samples (Shirovani et al. 1996). XANES measurements indicate trivalent Ce with strong hybridization with ligand orbitals. The gap is presumably formed from the hybridization of the Ce 4f states with the Ru d and P p orbitals (Kanai et al. 2002). The room temperature thermal conductivity of a dense polycrystalline

sample is 8.6 W/m-K (Watcharapasorn et al. 1999). The magnetic susceptibility is paramagnetic but relatively small at room temperature ( $\approx 0.001 \text{ cm}^3/\text{mole-Ce}$ ) and increases to about  $0.018 \text{ cm}^3/\text{mole}$  at 2 K (Shirotani et al. 1999). These values indicate a substantial reduction in the magnetism of the Ce 4f shell due to hybridization.

**CeOs<sub>4</sub>P<sub>12</sub>** is a narrow gap semiconductor with a gap of  $\approx 0.036 \text{ eV}$  ( $\approx 400 \text{ K}$ ) estimated from resistivity data (Shirotani et al. 1999). The room temperature resistivity is  $\approx 10^{-2} \Omega\text{-cm}$  increasing to  $\approx 10^4 \Omega\text{-cm}$  at 2 K. The magnetic susceptibility is similar to that of CeRu<sub>4</sub>P<sub>12</sub> (Shirotani et al. 1999). The as-grown samples are p-type with a room temperature Hall mobility of  $73 \text{ cm}^2/\text{V-sec}$  for a carrier concentration of  $5 \times 10^{19} \text{ cm}^{-3}$ . The room temperature values of the Seebeck coefficient and thermal conductivity are  $+147 \mu\text{V/K}$  and  $10.5 \text{ W/m-K}$ , respectively (Sekine et al. 2001).

**CeFe<sub>4</sub>As<sub>12</sub>** is probably a narrow gap semiconductor, but little low temperature data are available for this compound. The resistivity of a polycrystalline sample indicates a small gap on the order of  $0.01 \text{ eV}$  (Grandjean et al. 1984). The high temperature thermoelectric properties of this compound were investigated by Watcharapasorn et al. (2002). They found semimetallic behavior with a room temperature resistivity of  $0.49 \text{ m}\Omega\text{-cm}$ , a Seebeck coefficient of  $40 \mu\text{V/K}$ , and a thermal conductivity of  $3.8 \text{ W/m-K}$ . The maximum value for ZT, the thermoelectric figure of merit, was estimated to be 0.4 at 850 K.

**CeRu<sub>4</sub>As<sub>12</sub>** – only crystallography data has been reported for this compound (see table 1).

**CeFe<sub>4</sub>Sb<sub>12</sub>** is a moderately heavy fermion metal at low temperatures (Morelli and Meisner 1995, Gajewski et al. 1998, E. D. Bauer et al. 2000) and has excellent thermoelectric properties at elevated temperatures (Sales et al. 1996, Fleurial et al 1996, Sales et al. 1997). LDA calculations predict a small gap ( $0.1 \text{ eV}$ ) that is not observed experimentally (Nordstrom and Singh 1996). The hybridization between the Ce 4f and the Fe 3d and P p states at the Fermi energy is apparently not large enough to create a gap. XANES measurements (Grandjean et al. 2000) indicate a Ce valence of  $3 \pm 0.02$ , and iron Mössbauer data show no indication of magnetic order (Long et al 1999). All of the reported data are from polycrystalline samples. Analysis of the low temperature heat capacity and magnetization data are complicated by small amounts of impurity phases (Morelli and Meisner 1995, Chen et al. 1997, Gajewski et at. 1998). Analysis of the low temperature heat capacity data yields  $\gamma = 180 \text{ mj/mole-K}^2$  and  $\Theta_D \approx 250 \text{ K}$  (Gajewski et al. 1998). The resistivity of CeFe<sub>4</sub>Sb has an unusual “S” shape that is characteristic of many

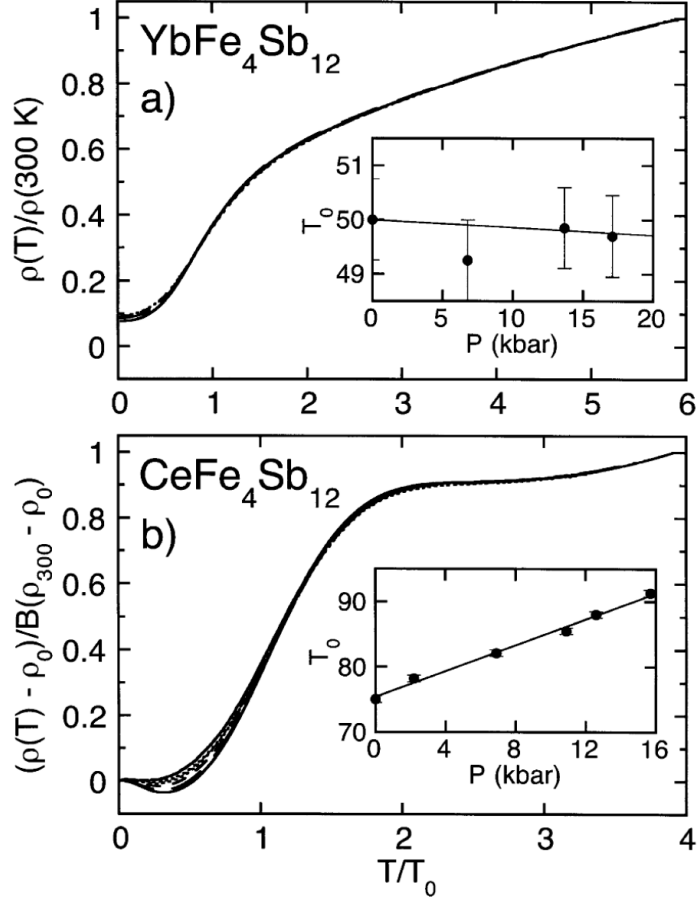


Fig. 9. (a) Scaled resistivity  $\rho(T)/\rho(300 \text{ K})$  versus  $T/T_0$  for  $\text{YbFe}_4\text{Sb}_{12}$ , where  $T_0$  is the scaling temperature. Inset shows the pressure dependence of  $T_0$ . (b) Scaled resistivity of  $\text{CeFe}_4\text{Sb}_{12}$  versus  $T/T_0$ . Inset shows pressure dependence of  $T_0$ . The room temperature resistivity of both compounds was about  $0.8 \text{ m}\Omega\text{-cm}$  at ambient pressure (E. D. Bauer et al. 2000).

concentrated Kondo compounds (fig. 9b). The rapid decrease in resistivity at about 100 K is caused by the coherent scattering of electrons from the lanthanide sublattice. The interpretation of the magnetic data is complicated by an enhanced Pauli contribution from the Fe (Ravot et al. 2001), a relatively high Kondo temperature,  $T_K$ , of about 100 K (Gajewski et al. 1998) and the crystal field splitting of the Ce 4f level in a cubic crystal field. In spite of these complications, it is clear that the value of the Wilson-Sommerfeld ratio  $R_w = (\chi_0/\gamma)(\pi^2 k_B^2/\mu_{\text{eff}}^2)$  is of the order unity as expected for heavy fermion systems (Wilson 1975). In the expression for  $R_w$ ,  $\chi_0$  is the extrapolated Pauli susceptibility at  $T=0$  ( $0.008 \text{ emu/mole Ce}$ ), and  $\mu_{\text{eff}}$  is the magnetic moment per Ce ion ( $2.54 \mu_B$ ).

**CeRu<sub>4</sub>Sb<sub>12</sub>** is an unusual metal that exhibits non-Fermi liquid (NFL) behavior in the low temperature specific heat, resistivity, and magnetic susceptibility measurements on single crystals (Takeda and Ishikawa 2000a,b, 2001, E. D. Bauer et al. 2001a). CeRu<sub>4</sub>Sb<sub>12</sub> may be near a ferromagnetic quantum critical point. The low temperature ( $T < 4$  K) specific heat (fig. 10) and magnetic susceptibility of CeRu<sub>4</sub>Sb<sub>12</sub> are well described by a logarithmic divergence or a power law in temperature. The characteristic temperature,  $T^*$ , that is associated with the maximum in the magnetic susceptibility and with the rapid drop in the resistivity is about 75 K. The low temperature carrier mass,  $m^*$ , estimated from heat capacity and optical studies, is about 85 times the free electron mass (Dordevic et al. 2001). Optical measurements are able to directly measure the pseudo-gap,  $\Delta$ , created by the hybridization between the Ce 4f states and the extended conduction band states. The mass enhancement scales as  $m^*/m_e = (\Delta/T^*)^2$  as predicted by theory (Millis et al. 1987). The low temperature resistivity data for CeRu<sub>4</sub>Sb<sub>12</sub> reported by Takeda and Ishikawa (2000a, 2000b, 2001) follows a power law in temperature ( $\rho \propto T^n$ ) with  $n = 1.65$ . A magnetic field greater than 2 T appears to restore Fermi liquid behavior ( $n=2$ ) for temperatures less than 1 K, as did the substitution of a small amount of La for Ce. The La-doping studies with suggests that the parent compound, CeRu<sub>4</sub>Sb<sub>12</sub>, is near a ferromagnetic quantum critical point.

In contrast, E. D. Bauer et al. (2001a) found that the electrical resistivity is sample dependent with some specimens exhibiting NFL behavior below 5 K. For these samples the application of magnetic fields up to  $H = 8$  T does not significantly change the non-Fermi liquid ground state. The low temperature transport properties of CeRu<sub>4</sub>Sb<sub>12</sub> crystals are clearly sensitive to small changes in composition or small concentrations of impurities in the starting materials.

**CeOs<sub>4</sub>Sb<sub>12</sub>** is a narrow gap semiconductor with the gap caused by the hybridization of the Ce 4f level with states near the Fermi energy. Transport data on small single crystals shows a weakly activated behavior corresponding to a gap of about 10 K (E. D. Bauer et al. 2001b). Heat capacity data give  $\gamma \approx 92$  mJ/mole-K<sup>2</sup> and  $\Theta_D = 304$  K. No magnetic order was found above 0.5 K. The temperature dependence of the magnetic susceptibility data suggests a relatively large crystalline electric field splitting (327 K) of the Ce 4f level.

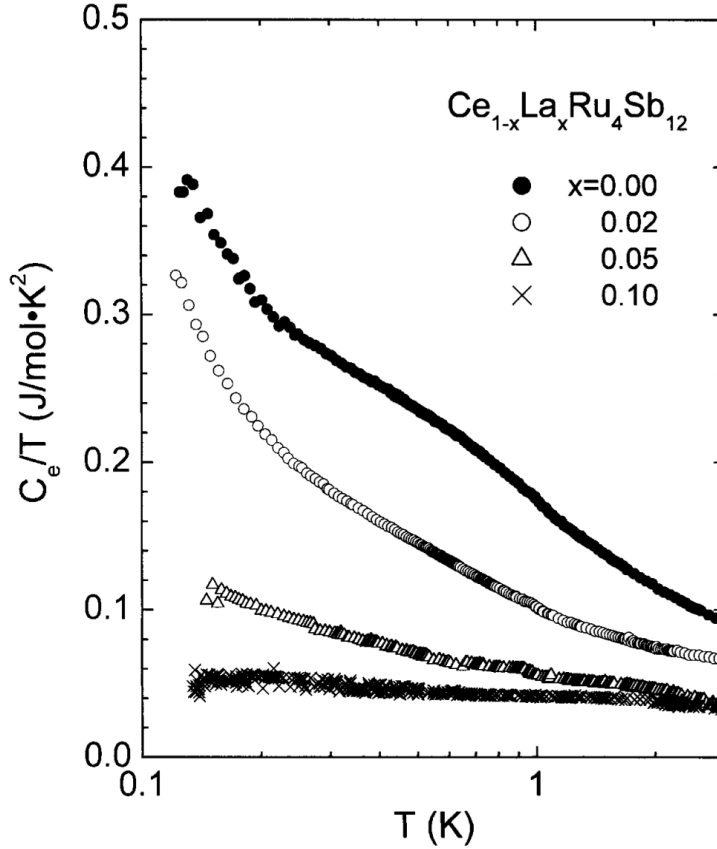


Fig. 10. Electronic contribution to the heat capacity divided by temperature versus  $\log_{10} T$  for a series of La doped alloys of  $\text{CeRu}_4\text{Sb}_{12}$ . The data has been corrected for a phonon contribution, using heat capacity data from  $\text{LaRu}_4\text{Sb}_{12}$ , and a nuclear quadrupolar contribution from  $^{121}\text{Sb}$  and  $^{123}\text{Sb}$  (Takeda and Ishikawa 2001).

## 7. Pr filled skutterudites

$\text{PrFe}_4\text{P}_{12}$  is quite an unusual compound that exhibits weak semiconducting behavior from 20-300 K followed by an even stranger phase transition near 5 K (fig. 11) (Sato et al. 2000a,b, Aoki et al. 2002). Originally it was thought that the low temperature phase transition corresponded to the onset of antiferromagnetic ordering of the Pr magnetic moments (Torikachvili et al. 1987). More recent work indicates that the phase transition probably corresponds to the ordering of the Pr quadrupole moments since for temperatures below the transition each Pr ion has a low magnetic moment implying a non-magnetic ground state ( $< 0.03 \mu_B/\text{Pr}$ ) (Aoki et al. 2002). No magnetic ordering is evident in neutron scattering measurements (Keller et al. 2001). The Hall coefficient changes by more than two orders of magnitude below 5

K but becomes temperature independent below 2 K. The Hall data suggests a gap structure similar to that seen in the resistivity (fig. 11) and heat capacity data. The Seebeck coefficient is extremely large below 5 K reaching a maximum value of  $-130 \mu\text{V/K}$  at 4 K, which reflects an

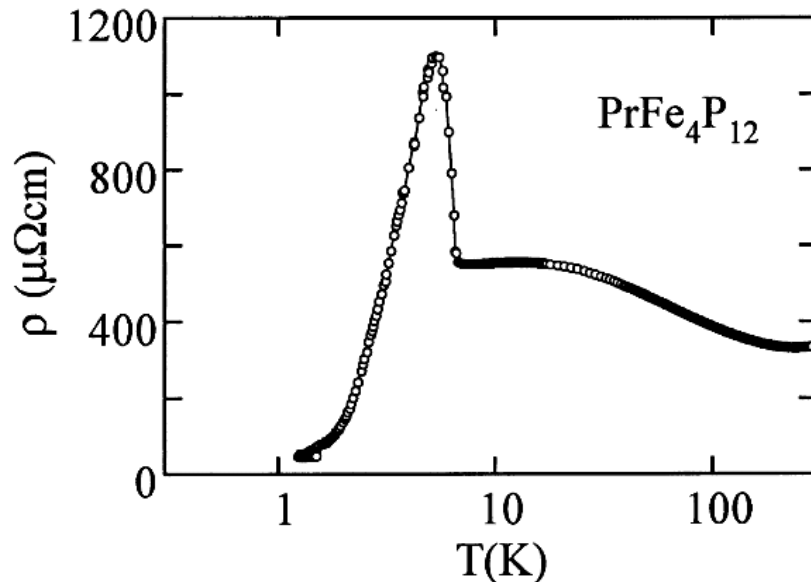


Fig. 11. Electrical resistivity vs.  $\log_{10}T$  for  $\text{PrFe}_4\text{P}_{12}$ . Below 3 K the resistivity is accurately described by  $\rho(T) = 20 + 273 T^2 \exp(-6.8/T)$ , corresponding to the temperature dependence of scattering with a gap structure (Sato et. al 2000a).

unusually sharp feature in the electronic density of states. The application of a magnetic field induces a transition to a heavy-fermion state (HFS) with a well-defined phase boundary as a function of magnetic field and temperature (figs. 12, 13). A metamagnetic phase transition (fig.14) is also associated with the phase boundary (Torikachvili et al. 1987, Matsuda et al. 2000, Aoki et al. 2002). It is suggested that the quadrupolar degrees of freedom are essential for the formation of the heavy-fermion state in this material. The crystalline electric field level schemes estimated from the anisotropy in the magnetization are consistent with this conjecture. The de Haas-van Alphen (dHvA) effect has been used to study the electronic structure of  $\text{PrFe}_4\text{P}_{12}$ . An enormously enhanced cyclotron effective mass of  $81 m_e$  was found in the HFS phase. In the low field ordered phase a dHvA branch with a mass of  $10 m_e$  was also observed (Sugawara et al. 2001).

$\text{PrRu}_4\text{P}_{12}$  exhibits an unusual metal-insulator transition (M-I) at about 60 K (fig. 15) (Sekine et al. 1997). There is no magnetic anomaly associated with this transition and originally it was thought there is no structural change associated with the M-I. A small structural transition was

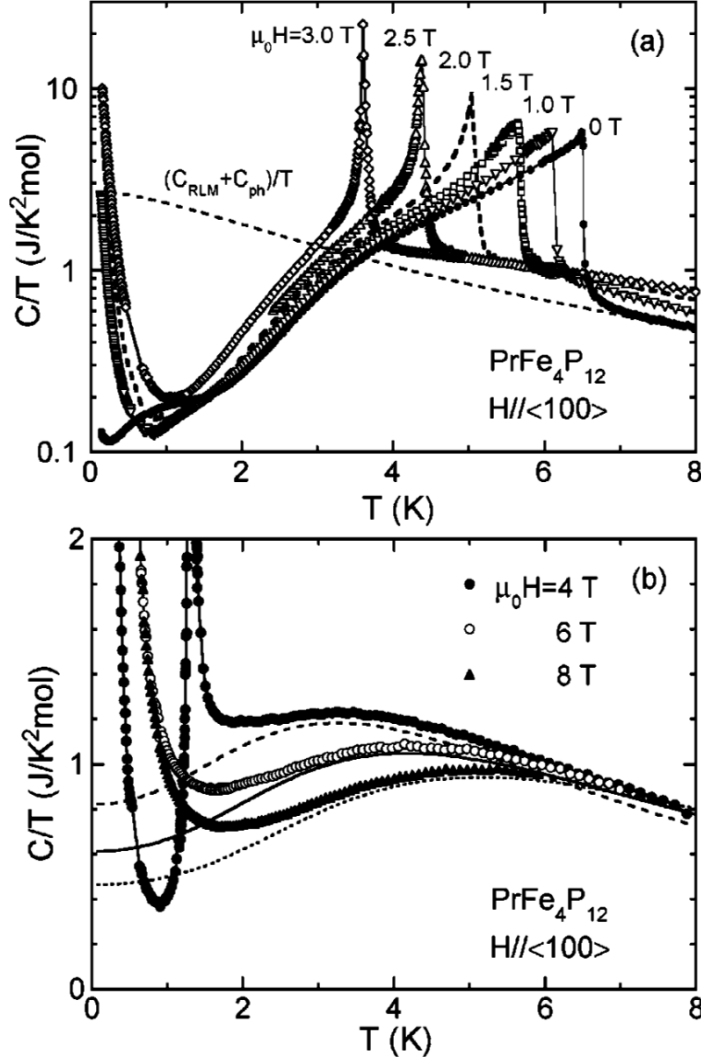


Fig. 12. Total heat capacity of a single crystal of  $\text{PrFe}_4\text{P}_{12}$  versus temperature in various applied magnetic fields: (a) low fields and (b) high fields. The dashed lines in (b) correspond to the best fit of the heavy fermion state to the resonant level model ( $C_{\text{RLM}}$ ).  $C_{\text{ph}}$  is the estimate of the phonon contribution to the heat capacity. (Aoki et al. 2002).

subsequently detected using electron diffraction in which the space group changes from  $\text{Im}\bar{3}$  (the skutterudite space group) to probably  $\text{Pm}\bar{3}$  (Lee et al. 2001). XANES measurements give a Pr valence of +3 for temperatures between 20 and 300 K, suggesting that there is no valence transition associated with the M-I (Lee et al. 1999). The opening of a gap at the Fermi energy (Nanba et al. 1999) is either due to a small displacement of the P atoms in the structure or perhaps charge ordering on the phosphorus (Lee et al. 2001). For temperatures near 60 K, Raman measurements on  $\text{PrRu}_4\text{P}_{12}$  indicate the softening of a mode at  $380\text{ cm}^{-1}$  that is associated with P vibrations (Sekine et al. 1999). There is a small jump in the thermal expansion coefficient at 63

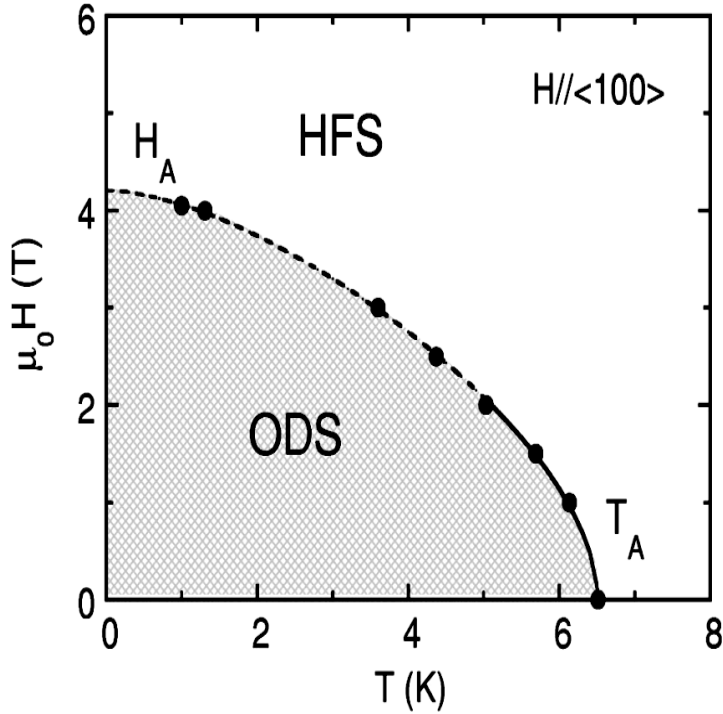


Fig. 13. Magnetic field versus temperature phase diagram of single crystal  $\text{PrFe}_4\text{P}_{12}$  with the magnetic fields applied along the (100) direction. The labels ODS and HFS refer to ordered state and heavy fermion state, respectively. The ordered state is probably due to quadrupolar ordering of the Pr 4f ground state. The solid and broken lines represent second-order and first-order phase boundaries, respectively. (Aoki et al. 2002)

$\text{K}$  ( $\approx 5 \times 10^{-7} \text{ K}^{-1}$ ) that shows no evidence of thermal hysteresis, indicating a second order phase transition. The thermal expansion anomaly is unaffected in magnetic fields up to at least 7 T (Matsushira et al. 2000). The magnetic susceptibility data follow a Curie-Weiss law at high temperatures with an effective moment of  $3.8 \mu_B$  and a Weiss temperature of  $-7 \text{ K}$ . The low temperature susceptibility ( $< 100 \text{ K}$ ) is complicated by the crystalline electric field at the Pr site that splits the  $J=4$  4f level (Sekine et al. 1997, 2000c). Heat capacity data suggest that the ground state of the Pr 4f shell is a  $\Gamma_3$  non-Kramers doublet. Antiferromagnetic order likely occurs for  $T < 0.35 \text{ K}$  (Meisner 1981).

$\text{PrOs}_4\text{P}_{12}$  is a metallic with a relatively temperature independent resistivity for temperatures between 50 and 300 K. Below 50 K there is a rapid drop in the resistivity similar to that observed in Pr metal or Kondo lattice Ce compounds such as  $\text{CeFe}_4\text{Sb}_{12}$  (fig. 9). There is also a small kink in the resistivity at 7 K of unknown origin. The magnetic susceptibility data follows a Curie-Weiss law at high temperatures with an effective moment of  $3.63 \mu_B$  and a Weiss temperature of

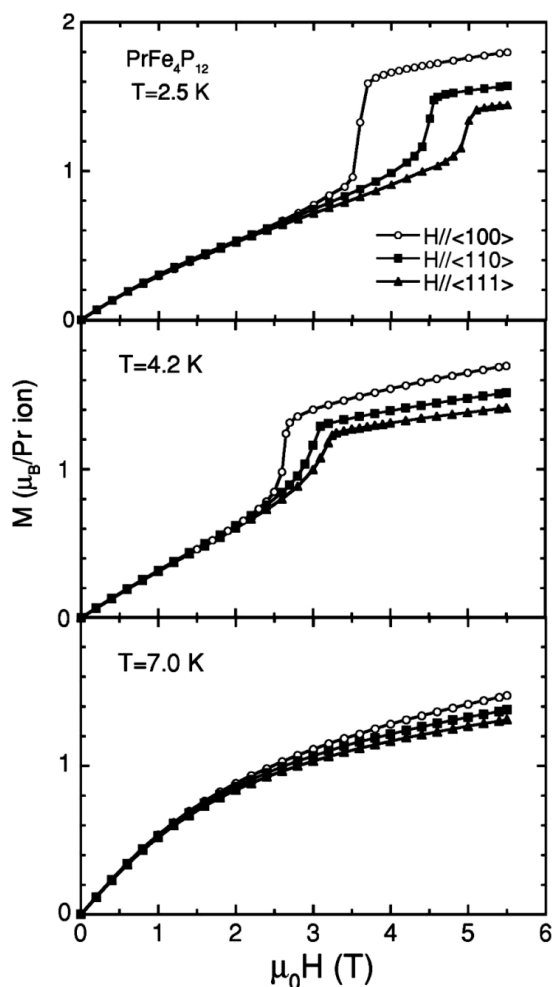


Fig. 14. Magnetization versus field at 2.5, 4.2 and 7 K with the magnetic field applied along the main symmetry directions of  $\text{PrFe}_4\text{P}_{12}$ . The observed magnetic anisotropy is a feature of the non-ordered state. (Aoki et al. 2002).

–17 K. There is no evidence for magnetic order above 1 K. Magnetization measurements at 2 K indicate a non-magnetic ground state caused by the crystalline electric field (Sekine et al. 1997).

**$\text{PrFe}_4\text{As}_{12}$**  – only crystallography data have been reported for this compound (see table 1).

**$\text{PrRu}_4\text{As}_{12}$**  is a superconductor below 2.4 K. The resistivity of a polycrystalline sample changes from 1 m $\Omega$ -cm at room temperature to 0.25 m $\Omega$ -cm at 3 K (Shirotani et al. 1997).

**$\text{PrOs}_4\text{As}_{12}$**  – only crystallography data have been reported for this compound (see table 1).

**$\text{PrFe}_4\text{Sb}_{12}$**  is likely a metal. Magnetic measurements on polycrystalline samples that were about 90% phase pure indicated ferromagnetic ordering below 5 K with a moment of 1 $\mu_B$  per

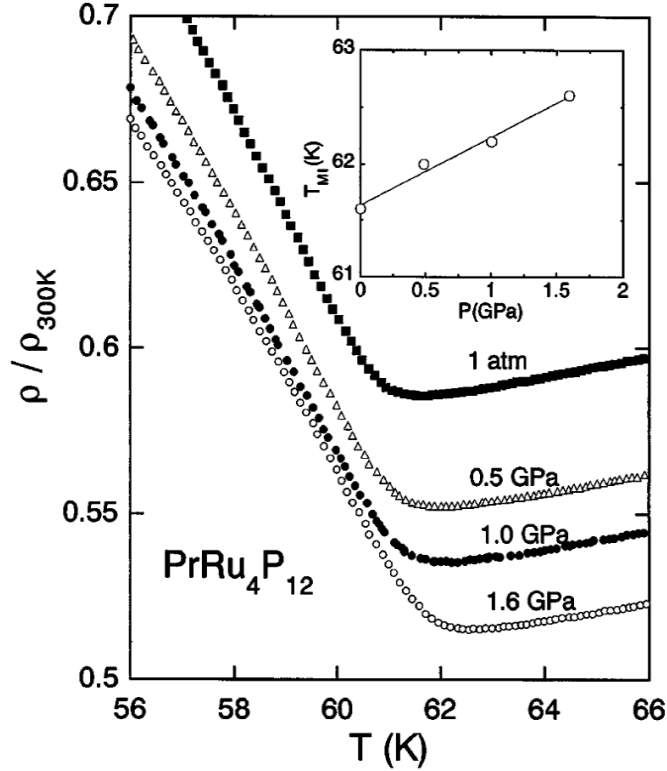


Fig. 15. Normalized resistivity of  $\text{PrRu}_4\text{P}_{12}$  versus temperature at pressures from 1 atm to 1.6 GPa (Sekine et al. 1997).

formula unit. The only other phase detected using x-ray diffraction was  $\text{FeSb}_2$ , which has a weak Pauli paramagnetic susceptibility (Dannebrock et al. 1996).

$\text{PrRu}_4\text{Sb}_{12}$  is a metal that becomes superconducting below 1 K. Heat capacity data confirm the bulk nature of the superconductivity with  $\Delta C/\gamma T_c = 1.87$ , which is larger than the 1.43 value expected from BCS theory. Values for  $\Theta_D$  and  $\gamma$  are 232 K and 59 mJ/mole- $\text{K}^2$  respectively. The magnetic susceptibility data indicates a non-magnetic ground state for the  $\text{Pr}^{+3}$  ions and a substantial crystal field splitting greater than 125 K (Takeda and Ishikawa 2000b).

$\text{PrOs}_4\text{Sb}_{12}$  is the first known example of a heavy-fermion superconductor containing Pr (E. D. Bauer et al. et al. 2002). Heavy-fermion behavior is inferred by the size of the jump in the heat capacity at  $T_c = 1.76$  K and by the slope of the critical field near  $T_c$ . Both analyses suggest  $\gamma \approx 350$  mJ/mole- $\text{K}^2$  and  $m^* \approx 100 m_e$ . The resistivity, magnetic susceptibility and heat capacity data are shown in fig. 16. The analysis of the data is complicated by the crystal electric field (CEF) splitting of the Pr levels 4f levels. The resistivity drops by almost a factor of 2 between 7 K and the onset of the superconducting transition at 1.76 K. In many lanthanide compounds this

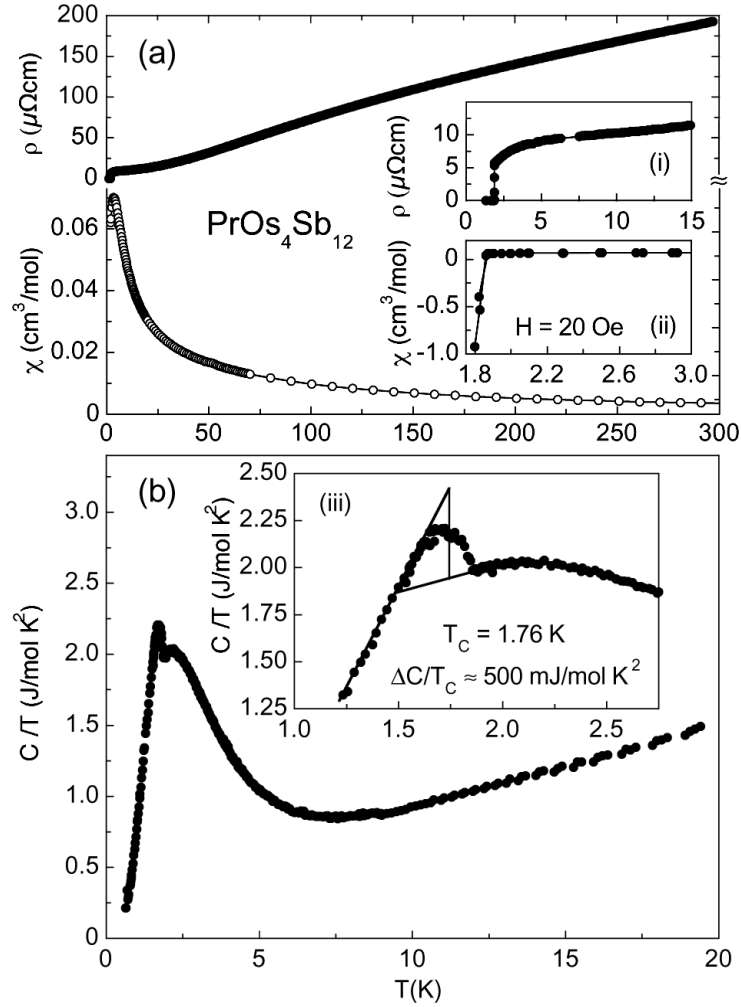


Fig. 16. (a) Resistivity and magnetic susceptibility, and (b) heat capacity data for  $\text{PrOs}_4\text{Sb}_{12}$  (E. D. Bauer et al. 2002).

drop is often indicative of low lying CEF levels. The broad Schottky like peak at 2.2 K is also consistent with this hypothesis. Quantitative fits to the magnetic susceptibility data plus an analysis of inelastic neutron scattering (Maple et al. 2002) and heat capacity data imply the  $J=4$   $\text{Pr}^{+3}$  level is split into a non-magnetic  $\Gamma_3$  doublet ground state, a  $\Gamma_5$  triplet at 8.2 K, a  $\Gamma_4$  triplet at 133 K and a  $\Gamma_1$  singlet at 320 K above the ground state. Heavy fermion behavior likely arises in this compound due to the interaction between the charge on the conduction electrons and fluctuations of the  $\text{Pr}^{+3}$  electric quadrupole moments associated with the  $\Gamma_3$  doublet ground state. The effect of  $\text{Pr}^{+3}$  quadrupole fluctuations on the superconductivity of  $\text{PrOs}_4\text{Sb}_{12}$  is an open question.

## 8. Nd filled skutterudites

**NdFe<sub>4</sub>P<sub>12</sub>** is metallic and orders ferromagnetically below 2K (Torikachvili et al. 1987). The resistivity decreases monotonically from a value of  $\approx 150 \mu\Omega\text{-cm}$  at room temperature to  $\approx 25 \mu\Omega\text{-cm}$  at 30 K. Below 30 K the resistivity increases with decreasing temperature (fig. 17) until the ferromagnetic phase transition is reached at 2 K. Below this transition the resistivity decreases as  $T^4$ , rather than the  $T^2$  expected from magnon scattering (Sato et al. 2000a,b). The heat capacity data below 2 K decreases as  $T^3$  rather than the  $T^{3/2}$  expected for a simple ferromagnet (Torikachvili et al. 1987). Both the heat capacity data and the resistivity can be understood if the magnon energy is linear in wavevector  $\mathbf{k}$  rather than proportional to  $\mathbf{k}^2$  (Sato et al. 2000a,b). The magnetic susceptibility follows a Curie-Weiss law for temperatures between 180 and 300 K with an effective moment of  $3.53 \mu_B$ , close to the  $\text{Nd}^{+3}$  free ion value of  $3.62 \mu_B$ . Below 150 K the positive curvature in the susceptibility indicates the effects of the CEF. Neutron scattering measurements have confirmed the ferromagnetic ordering of the Nd moments below 2 K (Keller et al. 2001). The ordered moment was found to be  $1.6 \mu_B$  at 1.5 K. De Hass van-Alfen measurements on  $\text{NdFe}_4\text{P}_{12}$  crystals showed a Fermi surface similar to  $\text{LaFe}_4\text{P}_{12}$  except for the splitting of the dHvA branches due to the ferromagnetic exchange interaction (Sugawara et al. 2000).

**NdRu<sub>4</sub>P<sub>12</sub>** is a metal that becomes ferromagnetic below 1.5 K (Sekine et al. 1998). Room temperature Raman data have been reported for this compound (Sekine et al. 1998). Three distinct Raman modes at  $370 \text{ cm}^{-1}$ ,  $385 \text{ cm}^{-1}$ , and  $415 \text{ cm}^{-1}$  were observed, but there was no detailed analysis of exactly which vibrations should be associated with these modes

**NdOs<sub>4</sub>P<sub>12</sub>** – only crystallography data have been reported for this compound (see table 1).

**NdFe<sub>4</sub>As<sub>12</sub>** – only crystallography data have been reported for this compound (see table 1).

**NdRu<sub>4</sub>As<sub>12</sub>** -has not been synthesized.

**NdOs<sub>4</sub>As<sub>12</sub>** – only crystallography data have been reported for this compound (see table 1).

**NdFe<sub>4</sub>Sb<sub>12</sub>** – only crystallography data have been reported for this compound (see table 1).

**NdRu<sub>4</sub>Sb<sub>12</sub>** is metallic and undergoes some type of magnetic transition near 1.3 K. The magnetic susceptibility follows a Curie-Weiss law above 50 K with an effective moment of  $3.45 \mu_B$  and a Weiss temperature of  $-28 \text{ K}$ . Crystal fields likely effect the susceptibility and magnetic

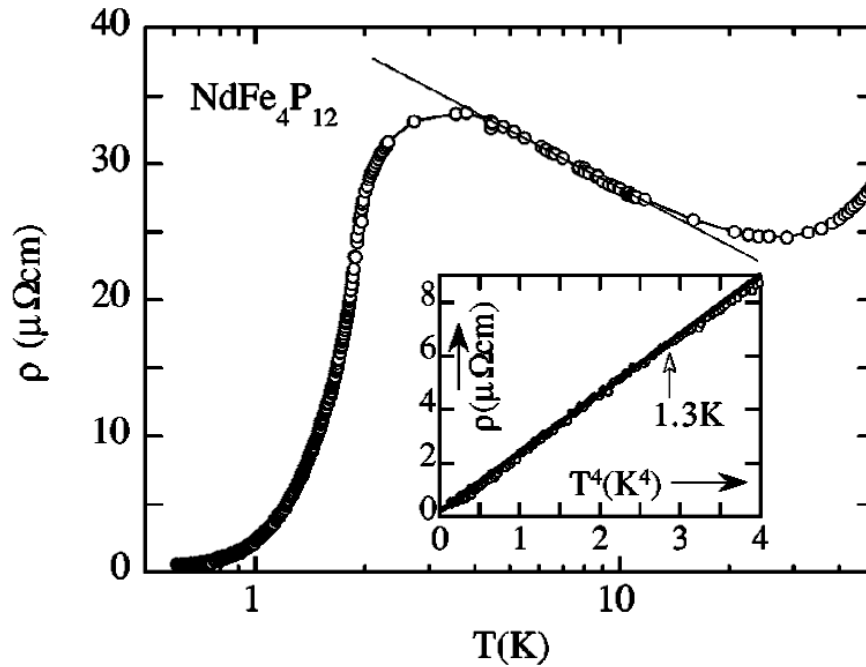


Fig. 17. Low temperature resistivity data for  $\text{NdFe}_4\text{P}_{12}$  (Sato et al. 2000b).

interactions for temperatures below 50 K. Low temperature heat capacity data confirm the bulk nature of the magnetic transition (Takeda and Ishikawa 2000b).

$\text{NdOs}_4\text{Sb}_{12}$  may undergo a displacive-type phase transition at  $-86^\circ\text{C}$  in which the Nd atoms freeze at off center positions (Evers et al. 1995). This transition was proposed on the basis of scanning calorimetry measurements and the huge room temperature value for the Nd atomic displacement parameter ( $B_{\text{eq}} = 4 \text{ \AA}^2$ ).

## 9. Sm filled skutterudites

$\text{SmFe}_4\text{P}_{12}$  is a metal that shows Van Vleck paramagnetism (Jeitschko et al. 2000).

$\text{SmRu}_4\text{P}_{12}$  undergoes a metal-to-insulator transition in conjunction with antiferromagnetic ordering at 16 K (Sekine et al. 1998).

$\text{SmFe}_4\text{Sb}_{12}$  is metallic and orders ferromagnetically for temperatures below 45 K with a relatively small saturation moment of  $0.7 \mu_B$  (Dannebrock et al. 1996).

$\text{SmRu}_4\text{Sb}_{12}$  and  $\text{SmOs}_4\text{Sb}_{12}$  – only crystallography data have been reported for these compounds (see table 1).

## 10. Eu filled skutterudites

**EuFe<sub>4</sub>P<sub>12</sub>** is metallic and orders ferromagnetically for temperatures below 100 K (Grandjean et al. 1984). The effective moment, as determined from the high temperature magnetic susceptibility data, is 6.2  $\mu_B$  per formula unit which is lower than the value expected for Eu<sup>+2</sup> of 7.94  $\mu_B$ . The hyperfine parameters as determined from Mössbauer spectroscopy are unusual. (Grandjean et al. 1983). The value of the Eu isomer shift in EuFe<sub>4</sub>P<sub>12</sub> is –6 mm/s and the isomer shift is independent of temperature from 4 K to 300 K. An isomer shift of –6 mm/s is near the limit for Eu<sup>+2</sup> compounds which suggests the possibility of a Eu valence that fluctuates between Eu<sup>+2</sup> and Eu<sup>+3</sup> configurations. If the Eu<sup>+3</sup> and Eu<sup>+2</sup> configurations are energetically degenerate, the average valence is determined by the degeneracy of each level, which implies a temperature independent valence of about  $3-8/9 = 2.11$ . Magnetic order in a mixed valence Eu compound would be extremely interesting. XANES measurements would be helpful in deciding if the Eu valence is intermediate in this material. The reduced moment for Eu<sup>+2</sup>, however, may simply indicate an incomplete filling of the lanthanide site.

**EuRu<sub>4</sub>P<sub>12</sub>** is metallic and orders ferromagnetically for temperatures below 18 K (Grandjean et al. 1983, Sekine et al. 2000b) The saturation moment is about 10% smaller than the Eu<sup>+2</sup> value of 7  $\mu_B$  which could imply an intermediate Eu valence or an incomplete filling of the lanthanide site. The value of the Eu isomer shift in EuRu<sub>4</sub>P<sub>12</sub> is –9.3 mm/s, which is compatible with Eu<sup>+2</sup> in a metallic compound.

**EuFe<sub>4</sub>Sb<sub>12</sub>** is metallic and ferromagnetic below 84 K (Dannebrock et al. 1996, E. Bauer et al. 2001a,b). The low temperature saturation moment, however, is only 64% (4.5  $\mu_B$ ) of the Eu<sup>+2</sup> value of 7  $\mu_B$  (Dannebrock et al. 1996, E. Bauer et al. 2001a,b). Part of the decrease is due to the incomplete filling of the Eu site (E. Bauer et al. 2001a,b) which was estimated to be 84%. The Eu Mössbauer isomer shift is –11.7 mm/s and is temperature independent, which clearly indicates divalent Eu. The remainder of the decrease in the saturation moment was attributed to some type of ferrimagnetism, possibly involving the Fe (E. Bauer et al. 2001a,b). The electrical resistivity is sensitive to the exact filling of the lanthanide site and the presence of impurity phases. The room temperature resistivity has been reported as low as 38  $\mu\Omega$ -cm (Bauer et al. 2001a,b) to 420  $\mu\Omega$ -cm (Kuznetsov and Rowe 2000). The samples of Kuznetsov and Rowe appear to be of higher quality and phase purity. The room temperature Seebeck coefficient is  $\approx$

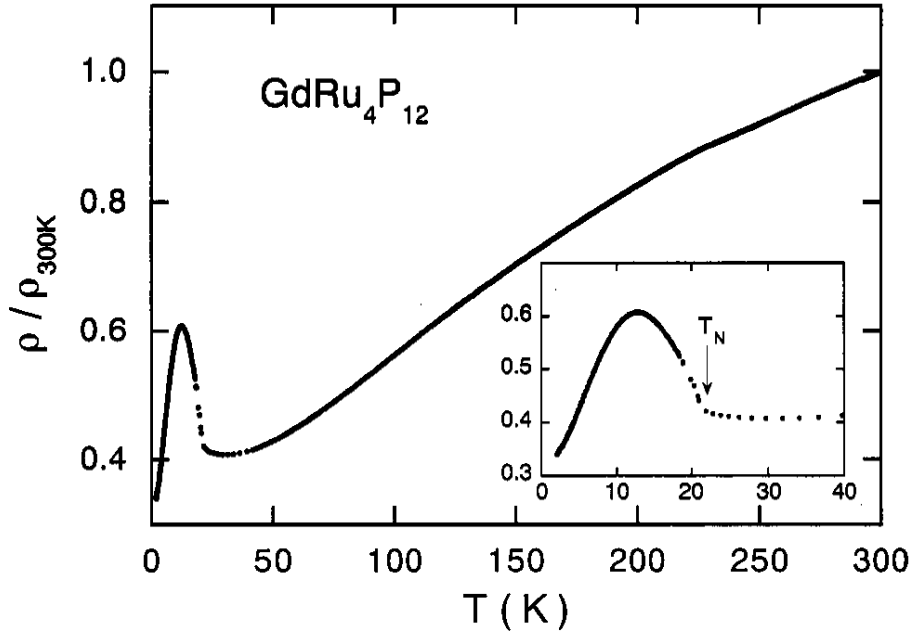


Fig. 18. Resistivity versus temperature for a polycrystalline sample of  $\text{GdRu}_4\text{P}_{12}$  synthesized using high pressures and temperatures (Sekine et al. 2000a).

60  $\mu\text{V/K}$  increasing to  $\approx 120 \mu\text{V/K}$  at 800 K (Kuznetsov and Rowe 2000). The thermoelectric properties of  $\text{EuFe}_4\text{Sb}_{12}$  are not promising.

**$\text{EuRu}_4\text{Sb}_{12}$**  is metallic and becomes ferromagnetic for temperatures below 3.3 K (Takeda and Ishikawa 2000b). The low temperature saturation moment is about  $6.2 \mu_B$ , 89% of the  $\text{Eu}^{+2}$  value. Low temperature heat capacity measurements indicate that the magnetic entropy removed due to magnetic order is also only about 90% of its expected value ( $R \ln 8$ ). It is likely that the lanthanide site is not completely filled in this compound although mixed valence behavior can not be ruled out with the available data.

### 11. Gd filled skutterudites

**$\text{GdFe}_4\text{P}_{12}$**  is metallic and a soft ferromagnet with a Curie temperature of 22 K (Jeitschko et al. 2000).

**$\text{GdRu}_4\text{P}_{12}$**  is metallic for temperatures between 30 K and 300 K, but undergoes an unusual phase transition near 20 K (fig. 18) (Sekine et al. 2000a). The magnetic susceptibility follows a Curie-Weiss law at high temperatures with effective moment of  $8.04 \mu_B$  and a Weiss Temperature of +22 K, which suggests ferromagnetic interactions. Below 22 K, however, the magnetization data are more consistent with a strange type of antiferromagnetic ordering. The

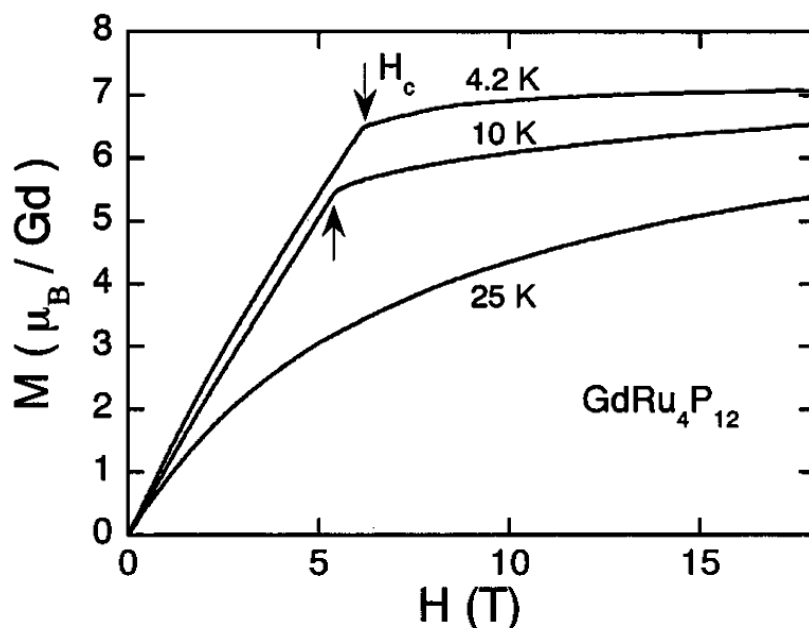


Fig. 19. Low temperature magnetization curves for  $\text{GdRu}_4\text{P}_{12}$  that indicate a field induced phase transition (Sekine et al. 2000a).

magnetization data also indicate a field-induced phase transition at low temperatures for magnetic fields  $\approx 5\text{-}6$  T. (fig 19).

## 12. Tb filled skutterudites

$\text{TbRu}_4\text{P}_{12}$  is metallic with unusual phase transitions at 20 K and 10 K (Sekine et al 2000a). The resistivity data from  $\text{TbRu}_4\text{P}_{12}$  is similar to that of  $\text{GdRu}_4\text{P}_{12}$  shown in fig. 18. The high temperature magnetic susceptibility data indicate ferromagnetic interactions (Weiss temperature  $\approx 8$  K) but low temperature data are more consistent with some type of antiferromagnetic order (fig. 20). Low temperature magnetization data indicate two metamagnetic phase transitions. It is possible that the unusual phase transitions at about 20 K in both  $\text{GdRu}_4\text{P}_{12}$  and  $\text{TbRu}_4\text{P}_{12}$  are related to the freezing of the lanthanide atoms in off-center positions.

## 13. Yb filled skutterudites

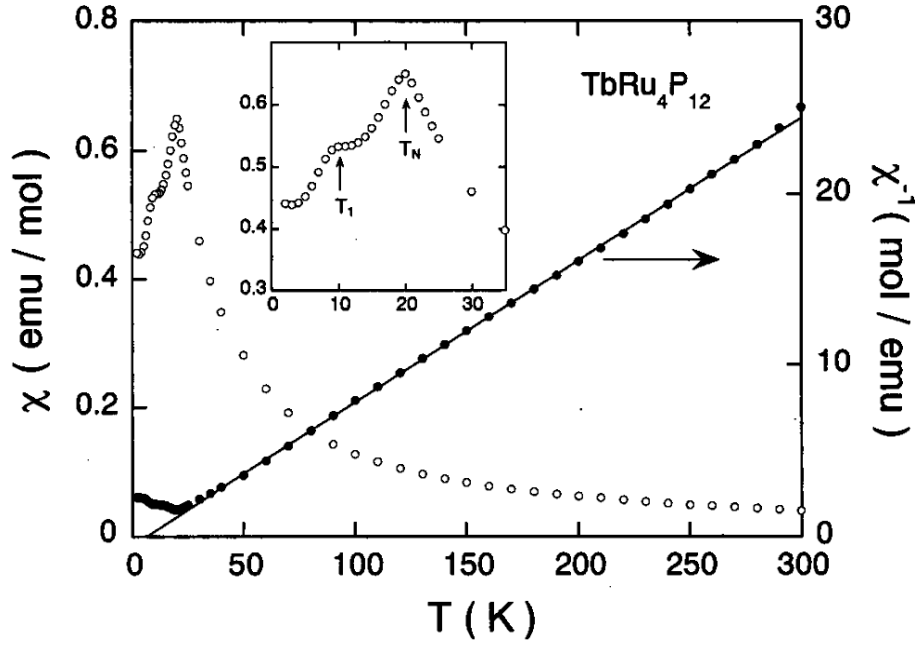


Fig. 20. Inverse magnetic susceptibility of  $\text{TbRu}_4\text{P}_{12}$  versus temperature measured at  $H = 1$  T. Inset shows an enlarged view of susceptibility data below 20 K (Sekine et al. 2000a)

$\text{YbFe}_4\text{Sb}_{12}$  was first synthesized by Dilley et al. (1998). Measurements of the lattice constant, magnetization, resistivity and heat capacity suggest an intermediate valence for the Yb ions. XANES measurements yield a Yb valence of 2.68 (Leithe-Jasper et al. 1999). The electronic specific heat coefficient is estimated to be  $\gamma = 140$  mJ/mole-K<sup>2</sup> which indicates that the effective mass of the conduction electrons is moderately enhanced at low temperatures. The characteristic temperature,  $T^*$ , for the Yb valence fluctuations is estimated to be 50 K (see fig. 9a). The Wilson-Sommerfeld ratio,  $R_w$ , is about 2.6 in good agreement with the value of  $R_w=2$  expected for a spin 1/2 Kondo effect. The room temperature value of the resistivity is  $\approx 450$   $\mu\Omega$ -cm as determined from resistivity and optical measurements (Dordevic et al. 2001) and decreases to  $\approx 40$   $\mu\Omega$ -cm at 2 K. Optical measurements also are able to directly measure the pseudogap,  $\Delta = 90$   $\text{cm}^{-1}$ , created by the hybridization between the Yb 4f states and the extended conduction band states (fig. 21) The mass enhancement scales as  $m^*/m_e = (\Delta/T^*)^2$  as predicted by theory (Millis et al. 1987). The thermoelectric properties of  $\text{YbFe}_4\text{Sb}_{12}$  were investigated by Dilley et al. (1998, 2000), and Kuznetsov and Rowe (2000). The maximum estimated value of ZT is 0.4 at 670 K.

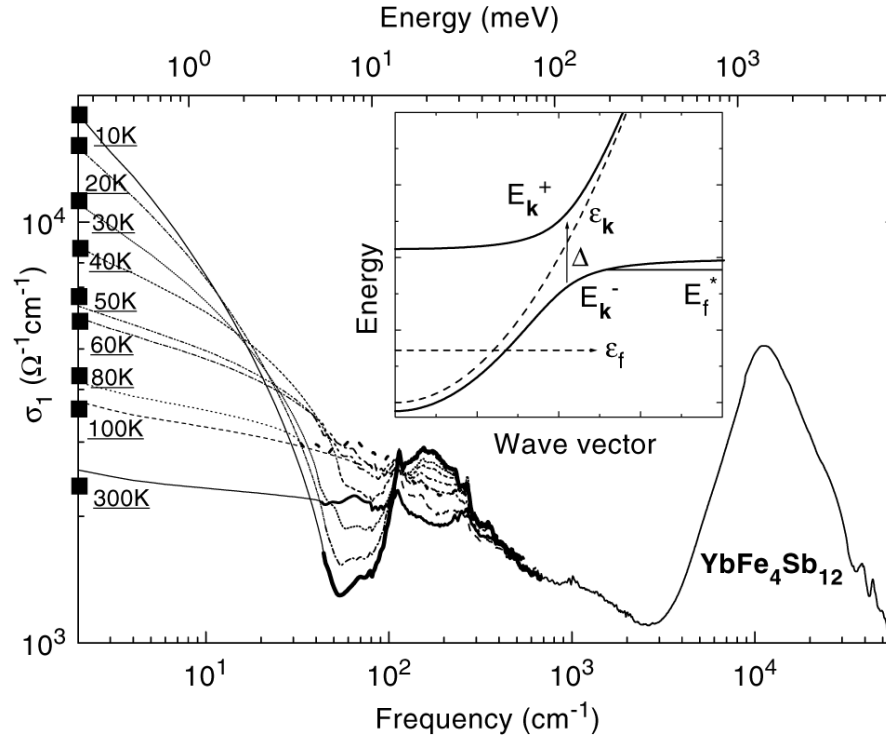


Fig. 21. Real part of the conductivity of  $\text{YbFe}_4\text{Sb}_{12}$ . The symbols on the left axis represent dc values at different temperatures. Below  $T^*$  ( $\approx 50$  K), a narrow peak at zero frequency and a gap-like feature at  $\approx 18$  meV gradually develop. Inset: Renormalized band structure calculated from the Anderson lattice Hamiltonian.  $\epsilon_k$  and  $\epsilon_f$  denote bands of free carriers and localized electrons, respectively. At low temperatures a direct gap  $\Delta$  opens. The Fermi level,  $E_F^*$  is near the top of the lower band,  $E_k^-$ , resulting in hole-like character and enhanced effective mass of the quasiparticles (Dordevic et al. 2001).

## 14. Filled Skutterudite thermoelectrics

### 14.1 Introduction to thermoelectric materials and devices

As mentioned in sect. 1, in 1996 it was found that some of the lanthanide antimony-based skutterudites had excellent thermoelectric properties above room temperature (Sales et al. 1996, Fleurial et al. 1996). This discovery greatly increased the interest in these materials for thermoelectric applications. In addition to the stoichiometric filled skutterudite compounds of the form  $\text{RM}_4\text{X}_{12}$ , a large number of related alloys were also investigated as possible thermoelectric materials. Most of the research on lanthanide skutterudites in the context of thermoelectric

applications has been reviewed recently by Uher (1999), Nolas et al. (1999), and Sales (1998) and hence only a brief summary of the thermoelectric research will be highlighted in this section.

In a solid that conducts both heat and electricity, the thermal and electrical currents are coupled together. This thermoelectric coupling can be used to construct devices that act as refrigerators, power generators or temperature sensors. The devices work because the electrons or holes in a conducting solid also carry heat as well as electrical charge. The electrical carriers are the “working fluid” in a thermoelectric refrigerator. Thermoelectric devices are attractive for many applications as they have no moving parts (except electrons and holes), use no liquid refrigerant and last indefinitely. The major disadvantage of thermoelectric devices is poor efficiency.

The efficiency of a thermoelectric solid is found to depend on material properties through the dimensionless parameter  $ZT$ :

$$ZT = TS^2/\rho\kappa \quad (1)$$

where  $T$  is the absolute temperature,  $\rho$  is the electrical resistivity,  $S$  is the Seebeck coefficient, and  $\kappa$  is the total thermal conductivity. The total thermal conductivity is often broken up into two parts,  $\kappa = \kappa_e + \kappa_L$  where  $\kappa_e$  is the heat carried by the electrons and holes and  $\kappa_L$  is the heat carried by the lattice.  $Z$  is defined as the figure of merit and  $ZT$  is often referred to as the dimensionless figure of merit. For power generation the efficiency is defined as heat in divided by work out and is given by:

$$\text{Efficiency} = (T_h - T_{co}) (\Gamma - 1) / (T_{co} + \Gamma T_h) \quad (2)$$

where  $T_{co}$  ( $T_h$ ) is the temperature of the cold (hot) end and  $\Gamma = (1+ZT)^{1/2}$  varies with the average temperature  $T$ . For refrigeration, efficiency is defined as the work in divided by the heat pumped out and is called the Coefficient of Performance (COP). The COP can be greater than 1 and is given by:

$$\text{COP} = (\Gamma T_{co} - T_h) / [(T_h - T_{co}) (1 + \Gamma)] \quad (3)$$

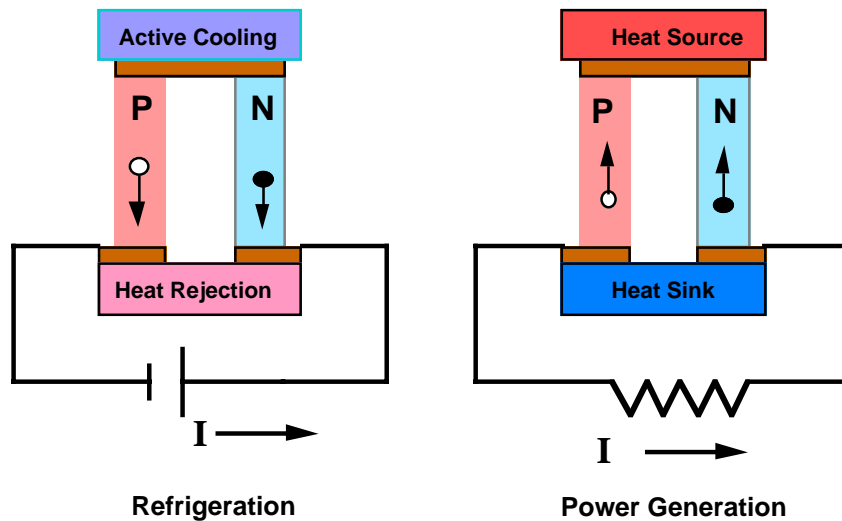


Fig. 22. A single thermoelectric couple is illustrated that has been configured for refrigeration or power generation. The labels "p" (positive) and "n" (negative) refer to the sign of the charge carriers in each leg (open circles correspond to holes and filled circles to electrons). Refrigeration is possible in these devices because electrons (or holes) carry heat, and hot electrons (holes) can be forced away from the cold end of the device by the battery. If a temperature difference is externally imposed on the device, useful power can be extracted.

For  $ZT \gg 1$ , Carnot efficiency is obtained for power generation and the Carnot limit to the COP is obtained for refrigeration. Materials currently used in thermoelectric devices have  $ZT$  values between 0.4 and 1.0.

All thermoelectric devices are composed of thermoelectric couples such as illustrated in fig. 22. Each leg of the couple is a doped semiconductor (or semimetal) with one p-type and one n-type leg. P-type (n-type) means that the dominant charge carriers are positive (negative). One side of the couple is thermally and electrically shorted together using a metal like copper (brown region). Electrical and thermal contact to a heat sink and the battery or load are made through copper pads at the open end of the couple (brown regions). Since the electrons and holes in a material carry heat, a battery can be used to force the hot electrons and holes away from the cold end of the device resulting in cooling of the cold end. If the direction of the current is reversed, the hot and cold ends are also reversed. If a temperature gradient is imposed across the thermoelectric couple, useful power can be extracted. In an actual thermoelectric device, typically several tens of these couples are connected together in series. For good general reviews

of thermoelectric devices, materials and theory refer to Rowe (1995), Goldsmid (1986), Mahan et al. (1997), Mahan (1998), Sales (2002), and Nolas et al. (2001).

#### **14.2 Electron crystals and phonon glasses**

In an ideal thermoelectric material the holes and electrons should have high mobilities and high effective masses. A high mobility and a high effective mass result in a large value of  $S^2/\rho$  (see equation 1 and Goldsmid 1986). High mobilities are typically found in crystals with a high degree of structural perfection. The ideal thermoelectric material should also have the lowest possible lattice thermal conductivity  $\kappa_L$ . The lowest possible value of  $\kappa_L$  for a particular solid is that of a glass with the same chemical composition,  $\kappa_{\min}$  (Slack 1979). The ideal thermoelectric material should therefore conduct electricity like a crystal but conduct heat like a glass. The skutterudite  $\text{CoSb}_3$  has good electronic properties and can be doped n or p type (Dudkin and Abrikosov 1959, Caillat et al. 1996). However, the room temperature lattice thermal conductivity of  $\text{CoSb}_3$  is  $\approx 10$  W/m-K, which is an order of magnitude too large for a good thermoelectric material. Slack (1995) suggested filling the voids in the skutterudite structure with weakly bound atoms that “rattle” about their equilibrium positions. He reasoned that heavy “rattlers” with low Einstein temperatures would be effective in scattering the low frequency acoustic phonons that carry most of the heat in a solid. The “rattlers” should therefore dramatically lower  $\kappa_L$ . What was not clear, however, was how the “rattlers” would alter the electronic conduction. Although the electronic properties of the skutterudite antimonides were somewhat degraded by the presence of various rattlers, there was an overall increase in ZT (Morelli and Meisner 1995, Sales et al. 1996, Fleurial et al 1996, Nolas et al. 2000, Tang et al. 2001). Representative thermoelectric data from various filled skutterudite antimonides are shown in figs. 23-26. Some of the arsenides and phosphides have been investigated for thermoelectric applications (Watcharapasorn et al. 1999, 2002), but in general these materials are limited by their  $\kappa_L$  values, which are significantly higher than the values for the antimonides. This is not surprising since a lower average mass usually implies a higher sound velocity and a higher  $\kappa_L$ .

#### **14.3 Future of filled skutterudites as thermoelectrics**

The filled skutterudite antimonides appear to represent excellent examples of electron-crystal, phonon-glass materials. The incoherent rattling of the loosely bound lanthanide atoms in these materials is inferred from the large values of the ADP parameters obtained in single-crystal

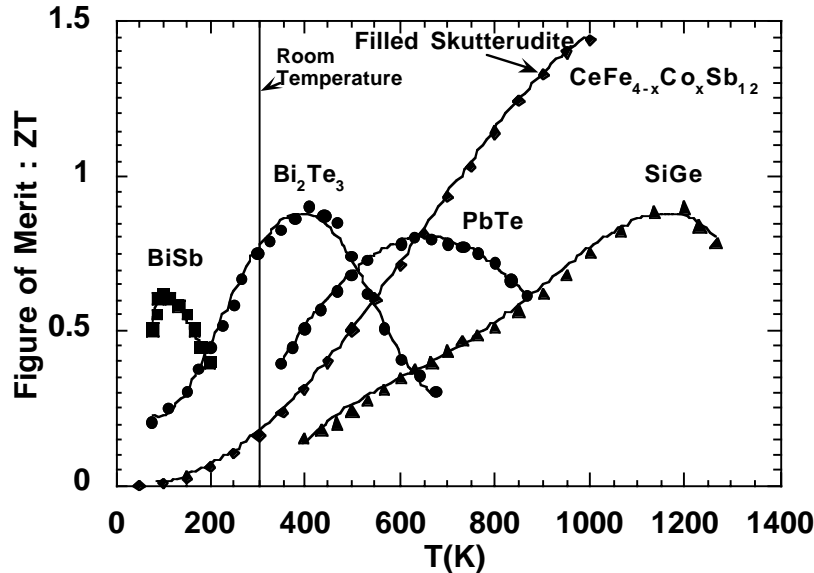


Fig. 23. ZT versus T for several state-of-the-art thermoelectric materials and for a filled skutterudite with  $x \approx 1$ . (Figure from T. M. Tritt, unpublished)

structure refinements. This rattling lowers the thermal conductivity at room temperature to values within two to three times  $\kappa_{\min}$ .

The electrical transport in the filled skutterudites is altered by the presence of the rattlers. Relative to the analogous unfilled compounds, the filled skutterudites exhibit larger effective masses and smaller mobilities. Good overall electrical transport is maintained as indicated by the large values of ZT at elevated temperatures (figs. 23-26). The high carrier concentrations in the filled skutterudites are due mostly to the fraction of the lanthanide sites that remain empty in samples prepared using equilibrium synthesis methods. A simple semiconductor transport model successfully reproduces most of the qualitative features of the resistivity and Seebeck data from these materials (Sales et al. 1997). By varying the extrinsic carrier concentration in the filled skutterudites, this model yields a maximum value for ZT of 1.4 at 1000 K, and a maximum ZT value of 0.3 at 300 K.

The ZT values of the filled skutterudites are too small for room temperature applications. The relatively large band gap of these compounds ( $\approx 0.6$  eV) makes it unlikely that further research

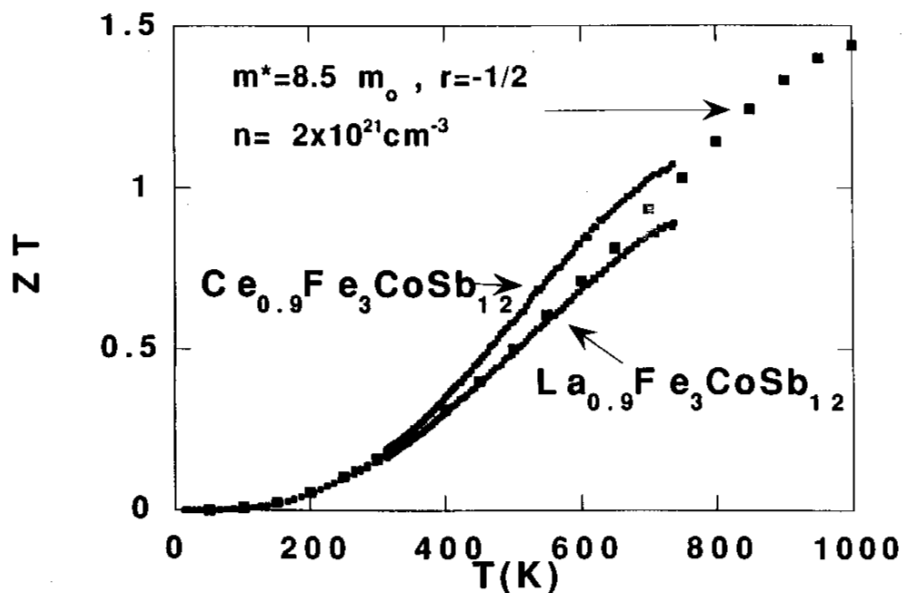


Fig. 24. ZT vs T for two rare-earth-filled skutterudites. Also shown are the results of a model calculation (squares) (Sales et al. 1997).

will result in a skutterudite-based thermoelectric material with properties better than the  $\text{Bi}_2\text{Te}_3$ -based materials currently in use near room temperature (see fig. 23). Only at temperatures in the 600-900 K temperature range are the thermoelectric properties of the filled skutterudite antimonides of interest for use in power generation applications. Thermoelectric generators using filled-skutterudite antimonides are being investigated by T. Caillat and collaborators at the Jet Propulsion Laboratory. These devices are of interest to NASA as a source of electrical power for deep space missions such as the Cassini and Voyager probes. Filled skutterudites may also be of practical use in the thermoelectric conversion of waste heat into useful electricity.

The filled skutterudite antimonides have demonstrated the validity of the "electron-crystal, phonon-glass" idea in the design of new thermoelectric materials for operation at elevated temperatures. There are many other crystal structures and compounds that contain atomic cages large enough to incorporate additional atoms. It is believed that the filled-skutterudite antimonides only represent a small fraction of a more general class of "rattling semiconductors" and that some of these materials will undoubtedly have high values of ZT at room temperature.

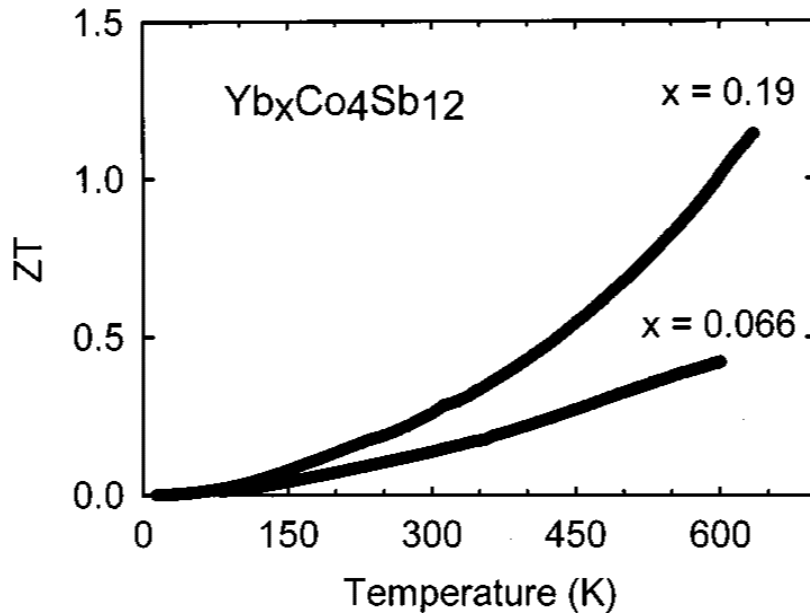


Fig. 25.  $ZT$  versus  $T$  for two Yb filled skutterudite samples (Nolas et al. 2000).

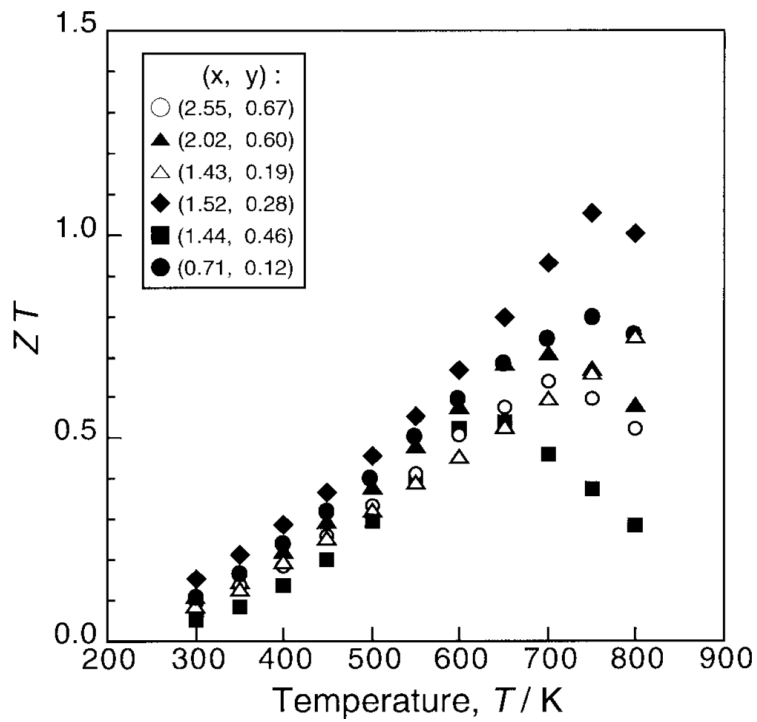


Fig. 26.  $ZT$  versus  $T$  for several filled skutterudite samples with the composition  $Ce_yFe_xCo_{4-x}Sb_{12}$  (Tang et al. 2001).

## 15. Concluding remarks

A major theme of contemporary solid state physics is focused on understanding the correlated behavior of electrons in solids. The challenge of this area was succinctly summarized by Anderson's title "more is different" (1972). The low temperature properties of the lanthanide-filled skutterudites touch on many of the exciting topics at the frontier of correlated electron physics.  $\text{CeFe}_4\text{Sb}_{12}$  and  $\text{YbFe}_4\text{Sb}_{12}$  are moderately heavy fermion metals.  $\text{CeRu}_4\text{Sb}_{12}$  exhibits non-fermi liquid behavior and may be near a ferromagnetic quantum critical point.  $\text{PrOs}_4\text{Sb}_{12}$  is the first example of a Pr compound that exhibits both superconductivity and heavy fermion behavior.  $\text{PrRu}_4\text{P}_{12}$  and  $\text{SmRu}_4\text{P}_{12}$  each undergo a metal-to-insulator transition and antiferromagnetic order.  $\text{PrFe}_4\text{P}_{12}$  is an extremely unusual material in which quadrupolar order (QO) and heavy fermion ground states are extremely close in energy. At low temperatures a magnetic field ( $\approx 4$  T) can drive  $\text{PrFe}_4\text{P}_{12}$  between the two ground states. The density of states in  $\text{PrFe}_4\text{P}_{12}$  is remarkably sharp in energy as evidenced by a two order of magnitude change in the Hall coefficient below 5 K and a huge value for  $S$  at 5 K of  $-130 \mu\text{V}/\text{K}$ . Most of the La-filled skutterudites and two of the Pr- filled skutterudites are superconductors with a maximum  $T_c$  of 10.3 K for  $\text{LaRu}_4\text{As}_{12}$ . Several of the Ce-filled skutterudites are narrow gap semiconductors (also called Kondo insulators) where the gap is created by a strong hybridization between the Ce 4f level and the transition metal and pnictogen states near the Fermi energy. The Nd, Eu, Gd and Tb filled skutterudites order magnetically at temperatures ranging from 2 K for  $\text{NdFe}_4\text{P}_{12}$  to 100 K for  $\text{EuFe}_4\text{P}_{12}$ . The coupling between the lanthanide magnetic moments and the conduction electrons is large in these compounds. This large coupling results in unusual peaks in electrical transport data near the onset of magnetic ordering, and in some cases multiple magnetic transitions. Finally, the thermoelectric figures of merit for the La, Ce and Yb filled skutterudites are among the highest values reported for any material at elevated temperatures (600-1000 K). It is hoped that this article has captured some of the excitement generated by the recent research on the lanthanide filled skutterudites.

## Acknowledgements

It is a pleasure to thank Peter Khalifah and Karl Gschneidner for many constructive comments and suggestions concerning both the science and the presentation of the work summarized in this

chapter. Oak Ridge National Laboratory is managed by UT-Battelle, LLC, for the U. S. Department of Energy under Contract No. DE-AC05-00OR22725.

Table 1. Crystallography data and ground state properties of filled skutterudites. Acronym Key: S = superconductor, HGS.= hybridization gap semiconductor, HFM = heavy fermion metal, M = metallic, NFL = non-Fermi-liquid, QCP = quantum critical point, QO = quadrupolar order, FIHF = field induced heavy fermion metal, FMM = ferromagnetic metal, AFM = antiferromagnetic metal, M-I = metal to insulating transition, AFM? = unusual magnetic phase transition,  $T_d$  = displacive transition. Reference key for crystallography data only: 1 = Jeitschko and Braun 1977, 2 = Braun and Jeitschko 1980a, 3 = Braun and Jeitschko 1980b, 4 = Braun and Jeitschko 1980c, 5 = Evers et al. 1995, 6 = Kaiser and Jeitschko 1999, 7 = Dilley et al. 1998, 8 = Stetson et al. 1991, 9= Jeitschko et al. 2000, 10 = Evers et al. 1994, 11= Sekine et al. 2000a

| Compound                           | Lattice Constant (Å) | Density (g/cm <sup>3</sup> ) (X-ray density) | Ground State/<br>Transition Temperature (K)      | Reference |
|------------------------------------|----------------------|--|--|-----------|
| LaFe <sub>4</sub> P <sub>12</sub>  | 7.8316               | 5.08   | S, T <sub>c</sub> =4.1                           | 1         |
| LaRu <sub>4</sub> P <sub>12</sub>  | 8.0561               | 5.81   | S, T <sub>c</sub> =7.2                           | 1         |
| LaOs <sub>4</sub> P <sub>12</sub>  | 8.0844               | 7.99   | S, T <sub>c</sub> = 1.8                          | 1         |
| LaFe <sub>4</sub> As <sub>12</sub> | 8.3252               | 7.26   | M  | 3         |
| LaRu <sub>4</sub> As <sub>12</sub> | 8.5081               | 7.77   | S, T <sub>c</sub> = 10.3                         | 3         |
| LaOs <sub>4</sub> As <sub>12</sub> | 8.5437               | 9.57   | S T <sub>c</sub> = 3.2                           | 3         |
| LaFe <sub>4</sub> Sb <sub>12</sub> | 9.1395               | 7.93   | M  | 2         |
| LaRu <sub>4</sub> Sb <sub>12</sub> | 9.2700               | 8.35   | S, T <sub>c</sub> = 2.8                          | 2         |
| LaOs <sub>4</sub> Sb <sub>12</sub> | 9.3029               | 9.74   | M  | 2         |
| CeFe <sub>4</sub> P <sub>12</sub>  | 7.7920               | 5.16   | HGS  | 1         |
| CeRu <sub>4</sub> P <sub>12</sub>  | 8.0376               | 5.86   | HGS  | 1         |
| CeOs <sub>4</sub> P <sub>12</sub>  | 8.0626               | 8.06   | HGS  | 1         |
| CeFe <sub>4</sub> As <sub>12</sub> | 8.2959               | 7.34   | -  | 3         |
| CeRu <sub>4</sub> As <sub>12</sub> | 8.4908               | 7.83   | -  | 3         |
| CeOs <sub>4</sub> As <sub>12</sub> | 8.5249               | 9.64   | -  | 3         |
| CeFe <sub>4</sub> Sb <sub>12</sub> | 9.1350               | 7.95   | HFM  | 2         |
| CeRu <sub>4</sub> Sb <sub>12</sub> | 9.2657               | 8.37   | NFL, QCP   | 2         |
| CeOs <sub>4</sub> Sb <sub>12</sub> | 9.3011               | 9.75   | HGS  | 2         |
| PrFe <sub>4</sub> P <sub>12</sub>  | 7.8149               | 5.12   | QO T <sub>QO</sub> = 6.5, FIHF                   | 1         |
| PrRu <sub>4</sub> P <sub>12</sub>  | 8.0420               | 5.86   | M-I T <sub>M-I</sub> = 60 , T <sub>AF</sub> ≈0.3 | 1         |
| PrOs <sub>4</sub> P <sub>12</sub>  | 8.0710               | 8.04   | M  | 1         |
| PrFe <sub>4</sub> As <sub>12</sub> | 8.3125               | 7.30   | -  | 3         |
| PrRu <sub>4</sub> As <sub>12</sub> | 8.4963               | 7.82   | S, T <sub>c</sub> =2.4                           | 3         |
| PrOs <sub>4</sub> As <sub>12</sub> | 8.5311               | 9.62   | -  | 3         |
| PrFe <sub>4</sub> Sb <sub>12</sub> | 9.1351               | 7.95   | FMM T <sub>FM</sub> =5                           | 2         |
| PrRu <sub>4</sub> Sb <sub>12</sub> | 9.2648               | 8.38   |  | 2         |
| PrOs <sub>4</sub> Sb <sub>12</sub> | 9.2994               | 9.76   | HFSC, T <sub>sc</sub> = 1.8                      | 2         |
| NdFe <sub>4</sub> P <sub>12</sub>  | 7.8079               | 5.16   | FMM T <sub>FM</sub> = 5                          | 1         |

|                                    |        |       |                               |    |
|------------------------------------|--------|-------|-------------------------------|----|
| NdRu <sub>4</sub> P <sub>12</sub>  | 8.0364 | 5.89  | FMM T <sub>FM</sub> = 1.5     | 1  |
| NdOs <sub>4</sub> P <sub>12</sub>  | 8.0638 | 8.09  | -                             | 1  |
| NdFe <sub>4</sub> As <sub>12</sub> | 8.309  | 7.39  | -                             | 9  |
| NdRu <sub>4</sub> As <sub>12</sub> | -      |       | -                             |    |
| NdOs <sub>4</sub> As <sub>12</sub> | 8.5291 | 9.65  | -                             | 3  |
| NdFe <sub>4</sub> Sb <sub>12</sub> | 9.130  | 8.04  | -                             | 5  |
| NdRu <sub>4</sub> Sb <sub>12</sub> | 9.2642 | 8.39  | AFM? T <sub>AF</sub> = 1.3    | 2  |
| NdOs <sub>4</sub> Sb <sub>12</sub> | 9.2989 | 9.77  | T <sub>d</sub> = 187          | 2  |
|                                    |        |       |                               |    |
| SmFe <sub>4</sub> P <sub>12</sub>  | 7.8029 | 5.21  | M                             | 1  |
| SmRu <sub>4</sub> P <sub>12</sub>  | 8.0397 | 5.96  | M-I & T <sub>AF</sub> = 16    | 11 |
| SmFe <sub>4</sub> Sb <sub>12</sub> | 9.130  | 8.06  | FMM T <sub>FM</sub> = 45      | 5  |
| SmRu <sub>4</sub> Sb <sub>12</sub> | 9.259  | 8.49  | -                             | 5  |
| SmOs <sub>4</sub> Sb <sub>12</sub> | 9.3009 | 9.79  | -                             | 2  |
|                                    |        |       |                               |    |
| EuFe <sub>4</sub> P <sub>12</sub>  | 7.8055 | 5.22  | FMM T <sub>FM</sub> = 100     | 1  |
| EuRu <sub>4</sub> P <sub>12</sub>  | 8.0406 | 5.93  | FMM T <sub>FM</sub> = 18      | 1  |
| EuFe <sub>4</sub> Sb <sub>12</sub> | 9.165  | 7.98  | FMM T <sub>FM</sub> = 84      | 5  |
| EuRu <sub>4</sub> Sb <sub>12</sub> | 9.2824 | 8.44  | FMM T <sub>FM</sub> = 3.3     | 2  |
| EuOs <sub>4</sub> Sb <sub>12</sub> | 9.3187 | 9.74  | -                             | 2  |
|                                    |        |       |                               |    |
| GdFe <sub>4</sub> P <sub>12</sub>  | 7.795  | 5.31  | FMM T <sub>FM</sub> = 22      | 9  |
| GdRu <sub>4</sub> P <sub>12</sub>  | 8.0375 | 6.01  | AFM? T <sub>AF</sub> = 21     | 11 |
|                                    |        |       |                               |    |
| TbRu <sub>4</sub> P <sub>12</sub>  | 8.0338 | 6.03  | AFM? T <sub>AF</sub> = 20, 10 | 11 |
|                                    |        |       |                               |    |
| YbFe <sub>4</sub> Sb <sub>12</sub> | 9.1580 | 8.09  | HFM, Mixed Valence            | 7  |
| YbOs <sub>4</sub> Sb <sub>12</sub> | 9.316  | 9.91  |                               | 6  |
|                                    |        |       |                               |    |
| ThFe <sub>4</sub> P <sub>12</sub>  | 7.7999 | 5.83  |                               | 4  |
| ThRu <sub>4</sub> P <sub>12</sub>  | 8.0461 | 6.47  |                               | 4  |
| ThOs <sub>4</sub> As <sub>12</sub> | 8.5183 | 10.24 |                               | 4  |
|                                    |        |       |                               |    |
| UFe <sub>4</sub> P <sub>12</sub>   | 7.7709 | 5.94  |                               | 5  |
| CaFe <sub>4</sub> Sb <sub>12</sub> | 9.162  | 7.5   |                               | 5  |
|                                    |        |       |                               |    |
| SrFe <sub>4</sub> Sb <sub>12</sub> | 9.1782 | 7.67  |                               | 10 |
| SrRu <sub>4</sub> Sb <sub>12</sub> | 9.2891 | 8.15  |                               | 5  |
| SrOs <sub>4</sub> Sb <sub>12</sub> | 9.322  | 9.52  |                               | 10 |
|                                    |        |       |                               |    |
| BaFe <sub>4</sub> Sb <sub>12</sub> | 9.200  | 7.82  |                               | 8  |
| BaRu <sub>4</sub> Sb <sub>12</sub> | 9.315  | 8.29  |                               | 5  |
| BaOs <sub>4</sub> Sb <sub>12</sub> | 9.3401 | 9.68  |                               | 10 |

## References

- Anderson, P. W., 1972 *Science* **177**, 393.
- Aoki, Y, T. Namiki, T. D. Masuda, K. Abe, H. Sugawara and H. Sato, 2002, *Phys. Rev. B.* **65**, 06446.
- Bauer, E., S. Berger, A. Galatanu, H. Michor, C. Paul, G. Hilscher, V. H. Tran, A. Grytsiv and P. Rogl, 2001a, *J. Mag. Magn. Mat.* **226-230**, 674.
- Bauer, E., St. Berger, A. Galatanu, M. Galli, H. Michor, G. Hilscher, Ch. Paul, Ch., B. Ni, M. M. Abd-Elmeguid, V. H. Tran, V.H.et. al., 2001b, *Phys. Rev. B.* **63**, 224414.
- Bauer, E.D., R. Chau, N. R. Dilley, M. B. Maple, D. Mandrus and B. C. Sales, 2000, *J. Phys. Cond. Mat.* **12**, 1261.
- Bauer, E.D., A. Slebarski, R. P. Dickey, E. J. Freeman, C. Sirvent, V. S. Zapf, N. R. Dilley and M. B. Maple, 2001a, *J. Phys. Cond. Mat* **13**, 5183.
- Bauer, E.D., A. Slebarski, E. J. Freeman, C. Sirvent, and M. B. Maple, 2001b, *J. Phys. Con. Mat.* **13**, 4495.
- Bauer, E. D., N. A. Frederick, P.-C. Ho, V. S. Zapf and M. B. Maple (2002), *Phys. Rev. B.* **65** 100506.
- Braun, D. J. and W. Jeitschko, 1980a, *J. Less Common Metals* **72**, 147.
- Braun, D. J. and W. Jeitschko, 1980b, *J. Solid State Chem.* **32**, 357.
- Braun, D.J. and W. Jeitschko, 1980c, *J. Less Common Metals* **76**, 33.
- Caillat, T, A. Borshchevsky, and J. -P. Fleurial, 1996, *J. Appl. Phys.* **80**, 4442.
- Chakoumakos, B.C., B. C. Sales, D. Mandrus and V. Keppens, 1999, *Acta Crystall. B.* **55**, 341.
- Chen, B., X. Jun-Hao, C. Uher, D. T. Morelli, G. P. Meisner, J.-P. Fleurial, T. Caillat, A. Borshchevsky, 1997, *Phys. Rev. B.* **55**, 1476.
- Corbett, J. D., 1985, *Chem. Rev.* **85**, 383.
- Dannebrock, M. E., C. B. H. Evers, and W. Jeitschko, 1996, *J. Phys. Chem. Solids* **57**, 381.
- Delong, L. E. and G. P. Meisner, 1985, *Solid State Commun.* **53**, 119.
- Dilley, N.R., E. J. Freeman, E. D. Bauer, and M. B. Maple, 1998, *Phys. Rev. B.* **58**, 6287.

- Dilley, N.R., E. D. Bauer, M. B. Maple, M.B. and B. C. Sales, 2000a, J. Appl. Phys. **88**, 1948.
- Dilley, N.R., E. D. Bauer, M. B. Maple, S. Dordevic, D. N. Basov, F. Freibert, T. W. Darling, A. Migliori, B. C. Chakoumakos, B.C. and B. C. Sales, 2000b, Phys. Rev. B. **61**, 4608.
- Dordevic, S. V., N. R. Dilley, E. D. Bauer, D. N. Basov, M. B. Maple 1999 Phys. Rev. B. **60**, 11321.
- Dordevic, S. V., D. N. Basov, N. R. Dilley, E. D. Bauer and M. B. Maple 2001 Phys. Rev. Lett. **86**, 684.
- Dudkin, L. D., and N. Kh. Abrikosov, 1959, Sov. Phys.-Solid State **1**, 126.
- Evers, C. B. H., L. Boonk and W. Jeitschko 1994, Z. Anorg. Allg. Chem. **620**, 1028
- Evers, C. B. H., W. Jeitschko, L. Boonk, D. J. Braun, T. Ebel, and U. D. Scholz, 1995, J. Alloys and Compounds **224**, 184.
- Feldman, J.L., D. J. Singh, I. I. Mazin, B. C. Sales and D. Mandrus, 2000, Phys. Rev. B. **61** R9209.
- Fleurial, J. -P, A. Borshchevsky, T. Caillat, D. T. Morelli and G. P. Meisner, 1996, Proc. 15<sup>th</sup> International Conference on Thermoelectrics, IEEE Catalog 96TH8169, Piscataway, NJ, p. 91.
- Gajewski, D.A., N. R. Dilley, E. D. Bauer, E. J. Freeman, R. Chau, M. B. Maple, D. Mandrus, B. C. Sales and A. H. Lacerda, 1998, J. Phys. Con. Mat. **10**, 6973.
- Goldsmid, H. J., 1986, *Electronic Refrigeration* (Pion Limited, London)
- Grandjean, F., A. Gerard, J. Hodges, D. J. Braun, D.J. and W. Jeitschko, 1983, Hyperfine Interactions **16**, 765.
- Grandjean, F., A. Gerard, D. J. Braun and W. Jeitschko, 1984, J. Phys. Chem. Solids **45**, 877.
- Grandjean, F., G. J. Long, R. Cortes, D. T. Morelli and G. P. Meisner, 2000, Phys. Rev. B. **62**, 12569.
- Harima, H., 1998 J. Magn. Magn. Mat., **177-181**, 321.
- Harima, H., 2000, Progress of Theoretical Physics Supplement; 2000; No. 138 p.117-18.
- Hornbostel, M. D., E. J. Hyer, J. H. Edvalson, D. C. Johnson, 1997a, Inorg. Chem. **36**, 4270.
- Hornbostel, M. D., E. J. HYer, J. Thiel, D. C. Johnson, 1997b, J. Am. Chem Soc. **119**, 2665.
- Jeitschko, W. and D. Braun, 1977, Acta Crystall. B **33**, 3401.

Jeitschko, W., A. J. Foecker, D. Paschke, M. V. Dewalsky, C. B. H. Evers, B. Kunnen, A. Lang, G. Kotzyba, U. C. Rodewald and M. H. Moller, 2000, *Z. Anorg. Allg. Chemie* **626**, 1112.

Kaiser, J.W. and W. Jeitschko, 1999, *J. Alloys and Compounds* **291**, 66.

Kanai, K, N. Takeda, S. Nozawa, T. Yokoya, M. Ishikawa, and S. Shin, 2002, *Phys. Rev B.* **65**, 041105(R).

Keller, L., P. Fischer, T. Herrmannsdorfer, A. Donni, H. Sugawara, T. D. Matsuda, K. Abe, Y. Aoki and H. Sato, 2001, *J. Alloys and Compounds* **323-324**, 516.

Keppens, V., D. Mandrus, B. C. Sales, B. C. Chakoumakos, P. Dai, R. Coldea, M. B. Maple, D. A. Gajewski, E. J. Freeman and S. Bennington, 1998, *Nature* **395**, 876.

Kuznetsov, V. L. and D. M. Rowe, 2000, *J. Phys. Cond. Mat.* **12**, 7915.

Lee, C. H., H. Oyanagi, C. Sekine, I. Shirotni, and M. Ishii, 1999, *Phys. Rev. B.* **60**, 13253.

Lee, C.H., H. Matsuhata, A. Yamamoto, T. Ohta, H. Takazawa, K. Ueno, C. Sekine, I. Shirotni and T. Hirayama, 2001, *J. Phys. Cond. Mat.* **13**, L45.

Leithe-Jasper, A., D. Kaczorowski, P. Rogl, J. Bogner, M. Reissner, W. Steiner, W. Wiesinger and C. Godart, 1999, *Solid State Commun.* **109**, 395.

Long, G.J., D. Hautot, F. Grandjean, D. T. Morelli and G. P. Meisner, 1999, *Phys. Rev. B.* **60**, 7410

Mahan, G., B. C. Sales and J. W. Sharp, 1997, *Physics Today*, March Issue pp. 42-47.

Mahan, G. D., 1998, *Solid State Physics*, Vol. 51 (Academic Press, San Diego), Chapter 2, pp. 81-157.

Maple, M.B., P. -C. Ho, V. S. Zapf, N. A. Frederick, E. D. Bauer, W. M. Yuhasz, F. M. Woodward, and J. W. Lynn, 2002, *J. Phys. Soc. Japan (supplement)*, **71**, 23.

Matsuda, T.D., H. Okada, H. Sugawara, Y. Aoki, H. Sato, A. V. Andreev, Y. Shiokawa, V. Sechovsky, T. Honma, E. Yamamoto, *et. al.*, 2000, *Physica B* **281-282**, 220.

Matsuhira, K., T. Takikawa, T. Sakakibara, C. Sekine and I. Shirotni, 2000, *Physica B.* **281-282**, 298.

Meisner, G. P., 1981, *Physica B* **108**, 763.

Meisner, G. P., M. S. Torikachvili, K. N. Yang, M. B. Maple, and R. P. Guertin 1985, *J. Appl. Phys.* **57**, 3073.

- Meisner, G.P., D. T. Morelli, S. Hu, J. Yang and C. Uher, 1998, Phys. Rev. Lett. **80**, 3551.
- Millis, A. J. et al. 1987, Phys. Rev. B. **35**, 3394.
- Morelli, D. T. and G. P. Meisner, 1995, J. Appl. Phys. **77**, 3777.
- Morelli, D.T., G. P. Meisner, B. Chen, S. Hu and C. Uher, 1997, Phys. Rev. B. **56**, 7376.
- Muller U., 1993, Inorganic Structural Chemistry (John Wiley and Sons, New York).
- Nanba, T., M. Hayashi, I. Shirovani and C. Sekine, 1999, Physica B **259-261**, 853.
- Nolas, G.S., G. A. Slack, T. Caillat, and G. P. Meisner, 1996a, J. Appl. Phys. **79**, 2622.
- Nolas, G.S., G. A. Slack, G.A., D. T. Morelli, T. M. Tritt and A. C. Ehrlich, 1996b, J. Appl. Phys. **79**, 4002.
- Nolas, G.S., J. L. Cohn, and G. A. Slack, 1998, Phys Rev. B. **58**, 164.
- Nolas, G. S., D. T. Morelli and T. M. Tritt, 1999, Ann. Rev. Mat. Sci. **29**, 89-116.
- Nolas, G.S., M. Kaeser, R. T. Littleton IV and T. M. Tritt, 2000, Appl. Phys. Lett. **77**, 1855.
- Nolas, G. S., J. Sharp and H. J. Goldsmid, 2001, *Thermoelectrics: Basic Principles and New Materials Developments* (Springer Verlag, New York)
- Nordstrom, L, and D. J. Singh, 1996, Phys. Rev. B. **53**, 1103.
- Oftedal, I 1928, Z. Kristallogr. **A66**, 517.
- Ravot, D., U. Lafont, L. Chapon, J. C. Tedenac, and A. Mauger, 2001, J. Alloys and Compounds **323**, 389.
- Rowe, D. M. (ed.) 1995, *CRC Handbook of Thermoelectrics* (Chemical Rubber Press, Boca Raton, FL).
- Sales, B. C., D. Mandrus and R. K. Williams, 1996, Science **272**, 1325.
- Sales, B.C., D. Mandrus, B. C. Chakoumakos, V. Keppens and J. R. Thompson, 1997, Phys. Rev. B. **56**, 15081.
- Sales, B. C., 1998 MRS Bulletin **23**, 15.
- Sales, B. C., B. C. Chakoumakos, D. Mandrus, and J. W. Sharp, 1999, J. Solid State Chem. **146**, 528.

- Sales, B.C., B. C. Chakoumakos and D. Mandrus, 2000, Phys. Rev. B. **61**, 2475.
- Sales, B. C, D. Mandrus and B. C. Chakoumakos, 2001a, Semiconductors and Semimetals, Vol. 70 (Academic Press, San Diego) Chapter 1, pp 1-36.
- Sales, B. C., B. C. Chakoumakos, R. Jin, J. R. Thompson and D. Mandrus, 2001b, Phys. Rev. B. **63**, 245113.
- Sales, B. C., 2002 Science **295**, 1248.
- Sato, H., Y. Abe, H. Okada, T. Matsuda, H. Sugawara and Y. Aoki, 2000 a, Physica B **281-282**, 306.
- Sato, H., Y. Abe, H. Okada, T. Matsuda, H. Sugawara and Y. Aoki, 2000 b, Phys. Rev. B. **62**, 15125.
- Sekine, C., T. Uchiumi, I. Shirotnani and T. Yagi, 1997, Phys. Rev. Lett. **79**, 3218.
- Sekine, C., H. Saito, T. Uchiumi, A. Sakai and I. Shirotnani, 1998, Solid State Commun. **106**, 441.
- Sekine, C., H. Saito, A. Sakai and I. Shirotnani, 1999, Solid State Commun. **109**, 449.
- Sekine, C., T. Uchiumi, I. Shirotnani, K. Matsuhira, T. Sakakibara, T. Goto and T. Yagi, 2000a, Phys. Rev. B. **62**, 11581.
- Sekine, C., M. Inoue, T. Inaba and I. Shirotnani, 2000b, Physica B. **281-282**, 308.
- Sekine, C., T. Inaba, I. Shirotnani, M. Yokoyama, H. Amitsuka and T. Sakakibara, 2000c, Physica B. **281-282**, 303.
- Sekine, C., K. Akita, N. Yanase, I. Shirotnani, I. Inagawa and Chul-Ho Lee, 2001, Jap. J. Appl. Phys. **40**, 3326.
- Shenoy, G.K., D. R. Noakes and G. P. Meisner, 1982, J. Appl. Phys. **53**, 2628.
- Shirotnani, I., T. Adachi, K. Tachi, S. Todo, K. Nozawa, T. Yagi, M. Kinoshita, 1996, J. Phys. Chem. Solids **57**, 211.
- Shirotnani, I., T. Uchiumi, K. Ohno, C. Sekine, Y. Nakazawa, K. Kanoda, S. Todo and T. Yagi, 1997, Phys. Rev. B. **56**, 7866.
- Shirotnani, I., T. Uchiumi, C. Sekine, M. Hori, S. Kimura and N. Hamaya, 1999, J. Solid State Chem. **142**, 146.

- Shirotani, I., K. Ohno, C. Sekine, T. Yagi, T. Kawakami, T. Nakanishi, H. Takahashi, J. Tang, A. Matsushita and T. Matsumoto, 2000, *Physica B.* **281-282**, 1021.
- Singh, D. J. and W. E. Pickett, 1994, *Phys. Rev. B.* **50**, 11235.
- Slack, G. A., 1979, *Solid State Physics*, Vol. 34 (Academic Press, New York), p. 1.
- Slack, G. A., 1995, *CRC Handbook of Thermoelectrics* (Chemical Rubber Company, Boca Raton Florida) pp. 407-440.
- Sofo, J. O., and G. D. Mahan, 1998, *Phys. Rev. B.* **58**, 15620.
- Stetson, N.T., S. M. Kauzlarich and H. Hope, 1991, *J. Solid State Chem.* **91**, 140.
- Sugawara, H., Y. Abe, Y. Aoki, H. Sato, M. Hedo, R. Settai, Y. Onuki and H. Harima, 2000, *J. Phys. Soc. Japan* **69**, 2938.
- Sugawara, H., T. D. Matsuda, K. Abe, K. Aoki, H. Sato, H., S. Nojiri, Y. Inada, R. Settai and Y. Onuki, 2001, *J. Mag. and Magnetic Mat.*, **226**, 48.
- Takeda, N. and M. Ishikawa, 2000a, *Physica B.* **281-282**, 388.
- Takeda, N and M. Ishikawa, 2000b, *J. Phys. Soc. Japan* **69**, 868.
- Takeda, N. and M. Ishikawa, 2001, *J. Phys. Cond. Mat.* **13**, 5971.
- Tang, X., L. Chen, T. Goto and T. Hirai, 2001, *J. Mat. Res.* **16**, 837.
- Torikachvili, M. S., J. W. Chen, Y. Dalichaouch, R. P. Guertin, M. W. McElfresh, C. Rossel, M. B. Maple, and G. P. Meisner, 1987, *Phys. Rev. B.* **36**, 8660.
- Uchiumi, T., I. Shirotani, C. Sekine, S. Todo, T. Yagi, Y. Nakazawa and K. Kanoda, 1999, *J. Phys. Chem. Solids* **60**, 689.
- Uher, C., 2000, *Semiconductors and Semimetals*, Vol. 69 (Academic Press, San Diego) Chapter 5, pp. 139-153.
- Watcharapasorn, A., R. C. DeMattei, R.S. Feigelson, T. Caillat, A. Borshchevsky, G. J. Snyder and J. -P. Fleurial, 1999, *J. Appl. Phys.* **86**, 6213.
- Watcharapasorn, A., R. S. Feigelson, T. Caillat, A. Borshchevsky, G. J. Snyder, J.-P. Fleurial, 2002, *J. Appl. Phys.* **91**, 1344.
- Wilson, K. G. 1975 *Rev. Mod. Phys.* **47**, 773.

Xue, J. S. M. A. Antonio, W. T. White, L. Soderholm, and S. M. Kauzlarich, 1994, *J. Alloys and Compounds*, **207-208**, 161.